IEEE Open Journal of
Industry Applications

Received 27 June 2020; revised 11 August 2020; accepted 25 August 2020. Date of publication 31 August 2020;
date of current version 23 September 2020. The review of this article was arranged by
Associate Editor L. Solero.

Digital Object Identifier 10.1109/OJIA.2020.3020392

Grid-Synchronization Stability of Converter-Based Resources—An Overview

XIONGFEI WANG [1] (Senior Member, IEEE), MADS GRAUNGAARD TAUL [1] (Member, IEEE), HENG WU [1] (Member, IEEE), YICHENG LIAO [1] (Student Member, IEEE), FREDE BLAABJERG [1] (Fellow, IEEE), AND LENNART HARNEFORS [2] (Fellow, IEEE)

(Invited Paper)

[1] Energy Technology, Aalborg University, Aalborg 9220, Denmark
[2] Energy Conversion, ABB Corporate Research Center Sweden, Vasteras N9C 4C2, Sweden

CORRESPONDING AUTHOR: XIONGFEI WANG (e-mail: xwa@et.aau.dk)

This work was supported by the Reliable Power Electronics-Based Power System (REPEPS) project at the Department of Energy Technology, Aalborg University, as a part of the Villum Investigator Program funded by the Villum Foundation.

ABSTRACT This paper presents an overview of the synchronization stability of converter-based resources under a wide range of grid conditions. The general grid-synchronization principles for grid-following and grid-forming modes are reviewed first. Then, the small-signal and transient stability of these two operating modes are discussed, and the design-oriented analyses are performed to illustrate the control impact. Lastly, perspectives on the prospects and challenges are shared.

INDEX TERMS Grid-Synchronization, sideband oscillations, phase-locked loops, transient stability, voltage-source converters.

I. INTRODUCTION

The past few years have witnessed an exponential growth of power-electronics-based resources in electric grids [1]. Differing from synchronous machines, the converter-based resources have no inherent 'swing equation' governing their synchronizations with the grid, but rather rely on digital control algorithms [2]. Therefore, the grid-synchronization dynamics of converter-based resources can be fundamentally different from synchronous machines.

A wide variety of grid-synchronization methods have been developed for converter-based resources [3]–[7]. The focus of research on the grid synchronization has been shifted from the rejection of disturbances, such as voltage harmonics and imbalances, phase jumps, and frequency deviations [3]–[5], to the synchronization stability in weak and faulty grids [6], [7]. This change has been driven by the ever-increasing share of converter-based resources in the power system, where the decreased inertia and the lowered short-circuit ratio (SCR) deteriorate the stability of converter-based resources [8].

Generally speaking, the grid synchronization methods can be classified into two categories with respect to the operating modes of converter-based resources:

1) *The voltage-based grid synchronization* that measures or estimates (voltage sensor-less) the frequency and phase of the voltage at the point of common coupling (PCC) of grid-connected converters. The detected phase is then used with the vector current control [4] or the direct power control [3] for regulating the active and reactive power exchanged with the grid. Such a voltage-based grid synchronization control is named as the grid-following control, since they follow the phase of grid voltage [9].
2) *The power-based synchronization* dictates directly the phase of the PCC voltage by regulating the active power of the converters [10], where the general idea is to utilize the active power-frequency (P-ω) droop control, which is widely used with synchronous generators, to synchronize converters with the grid [11]. To track the generated phase of the PCC voltage, the voltage control is

required, which, thus, differs from grid-following converters. Such voltage-controlled converters are recently known as the grid-forming converters [9], [12].

The stability implications of these two categories of grid synchronization methods are different. The synchronization stability of converter-based resources can be categorized into two types: small-signal stability and large-signal (transient) stability, similarly to the rotor angle stability of synchronous generators in legacy power systems [13].

The small-signal synchronization stability entails the ability of converter-based resources to maintain synchronism with the grid under small disturbances [6]. The disturbance is so small that the system dynamics can be linearized around the equilibrium point of interest, and thus the linear systems theory can be used for the dynamic analysis [13]. The small-signal analysis is widely used to evaluate the robustness of synchronization dynamics with different grid strengths. It is reported that the voltage-based synchronization methods, e.g. the phase-locked loop (PLL) that is commonly found in grid-following converters, can induce sideband oscillations around the grid fundamental frequency in low SCR grids [6], [8], [14], [15]. In contrast, the power-based synchronization algorithms used with grid-forming converters can result in sideband oscillations in stiff grids [16]–[20] and series compensated grids [21].

During large disturbances such as severe grid faults and loss of a large generation/load, the small-signal analysis will be inadequate to characterize the synchronization dynamics of converter-based resources, since the equilibrium points of the system may be changed or even lost in those scenarios. It is, thus, necessary to check first the presence of equilibrium points after the disturbance. Certainly, converters will lose the synchronism with the grid if no equilibrium points exist. However, even if there are equilibrium points after the large disturbance, converters may still lose the synchronism with the grid, since the system dynamics may not converge to the stable equilibrium point, which is highly dependent on the used grid-synchronization methods [22]–[26]. Therefore, the presence of equilibrium points is only a necessary condition for the transient stability of converter-based resources [7]. The nonlinear systems theory is required to evaluate if the system dynamics can converge to a stable equilibrium point when subjected to large disturbances. It has recently been found that the PLL essentially introduces a second-order nonlinear swing equation to grid-following converters, and a voltage-angle curve, instead of the conventional power-angle curve, is resulted for the transient stability analysis [22]. In contrast, the droop-controlled grid-forming converters can be characterized as a first-order nonlinear system, which can significantly improve the transient stability [23]. Yet, the reactive power droop control loop can adversely affect the transient stability of grid-forming converters [24]. Differing from synchronous generators (SGs), the limited overcurrent capability of power converters necessitates the use of current limiting control [12], which imposes another constraint to the transient stability behavior of grid-forming converters [25].

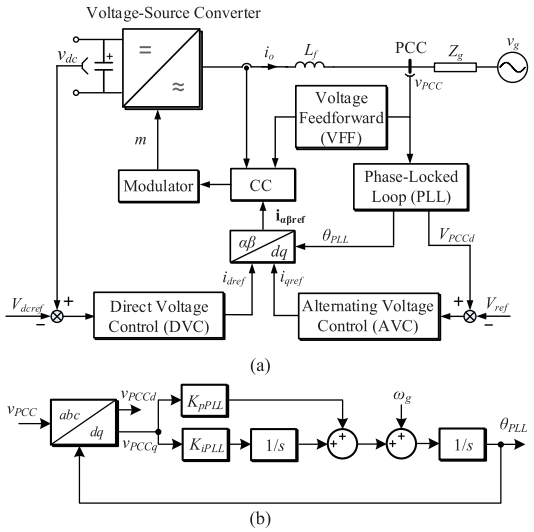

FIGURE 1. System diagram of a grid-following converter. (a) Main circuit and control system structure; (b) Phase-Locked Loop (PLL).

This paper intends to provide a systematic overview of the grid-synchronization stability of converter-based resources. The basics of grid-synchronization control are reviewed first in Section II, where the typical control topologies of grid-following and grid-forming converters are discussed, and the static power transfer limitations are analyzed to identify the presence of equilibrium points. Then, both the small-signal and transient stability of grid-following converters, as well as stabilization methods are addressed in Section III. This is followed by the stability characteristics and enhancement methods for grid-forming converters in Section IV. Section V concludes the paper with the challenges on grid codes and the prospects for future research.

II. BASICS OF GRID-SYNCHRONIZATION CONTROL

A. GRID-FOLLOWING CONVERTERS

Fig. 1 shows a control diagram of a grid-following converter [26]. The typical vector current control is adopted. The PLL plays a vital role in the synchronization of the grid-following converter; its diagram is shown in Fig. 1(b) [27]. With the transformation of the voltage vector in the dq frame and the regulation of the q-axis voltage by a proportional + integral (PI) controller, a feedback control loop is used to obtain the phase angle of the PCC voltage (v_{PCC}).

With the phase angle of v_{PCC}, the vector current control can also be oriented into the voltage dq-reference frame. The Direct Voltage Control (DVC) and the Alternating Voltage Control (AVC) can be utilized in the outer loops to generate the active-power and reactive-power current references by i_{dref} and i_{qref}, respectively. Consequently, the magnitude and phase of the current reference can be determined, and the current control can be implemented in the inner loop in either the $\alpha\beta$-reference frame or dq-reference frame. Also, the voltage feedforward (VFF) control is usually used through a low-pass

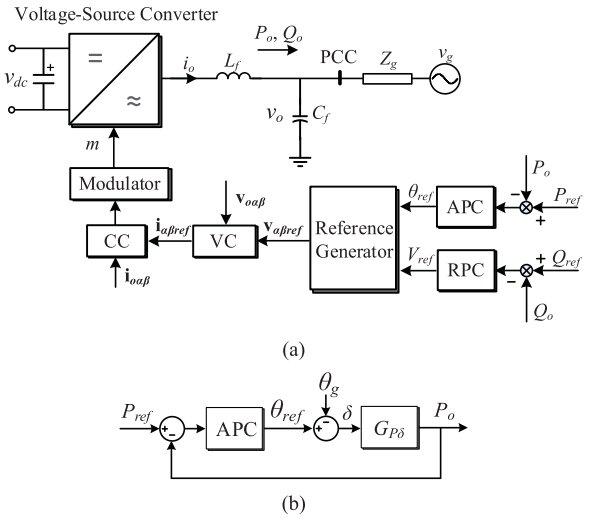

FIGURE 2. System diagram of a grid-forming converter. (a) Main circuit and control system structure. (b) Active Power Control (APC).

filter and added to the output of the current controller, to enhance the dynamic performance.

B. GRID-FORMING CONVERTERS

Fig. 2(a) shows a general system diagram of the grid-forming converter [10]. The output active and reactive powers of the grid-forming converter are regulated through the active and reactive power controls (APC and RPC) to generate the phase angle and voltage magnitude of the voltage reference, $\boldsymbol{v}_{\alpha\beta ref}$. The inner voltage control (VC) loop is used to regulate the output voltage of the converter, which is further cascaded with the current control (CC) loop for the overcurrent limitation and the LC filter resonance damping [28]. Differing from grid-following converters, a grid-forming converter behaves as a voltage source, which synchronizes with the power grid through the APC, as shown in Fig. 2(b). Hence, the PLL is not used for the grid-synchronization of grid-forming converters during normal operations [10], [29].

Fig. 3 shows four typical schemes of APC and RPC, which are 1) the power synchronization control (PSC) [10], 2) the basic droop control [28], 3) the droop control using low-pass filter (LPFs) [30], and 4) the basic virtual synchronous generator (VSG) control [31], [32]. The PSC and the basic droop control are equivalent to each other, and they can be categorized as the first-order power control [24]. The so-called "virtual inertia" can be synthesized by adding the LPF into the basic droop control, which has been proven equivalent to the basic VSG control [33], and they are categorized as the second-order power control. Further, since the first-order power control can be seen as a special case of the second-order one without inertial emulation, a general second-order power control model can be used to characterize the dynamics of grid-forming converters [24]. Hereafter, the droop control with LPFs is selected as the representative for the further analysis.

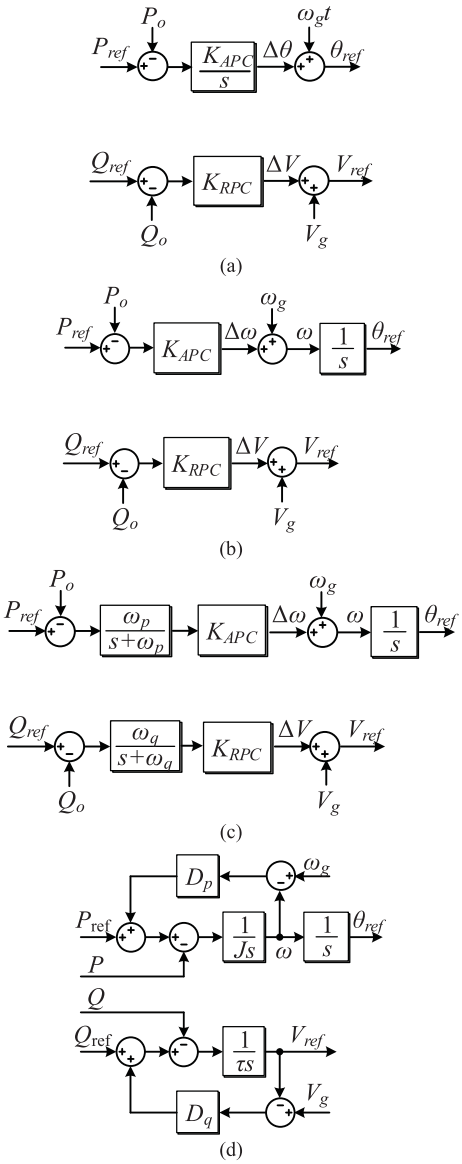

FIGURE 3. Typical schemes of APC and RPC. (a) PSC. (b) Basic droop control. (c) Droop control with LPFs. (d) VSG control [24].

It is worth mentioning that many alternative VSG control schemes have been recently introduced, in addition to the basic VSG control illustrated in Fig. 3(d). For example, an additional damping correction loop is reported in [34], which provides one more degree of freedom to adjust the damping ratio of VSG without affecting its steady-state frequency droop characteristic. In [35], the power system stabilizer (PSS) is added in the reactive power control of VSG for the stability enhancement. While these additional control loops bring in add-on benefits, their core control principle still follow the second-order swing equation of SGs, whose dynamic plays a critical role in the transient stability analysis.

C. STATIC POWER TRANSFER LIMITATION

During weak and faulty grid conditions, the synchronization instability will be inevitable when the converter violates the

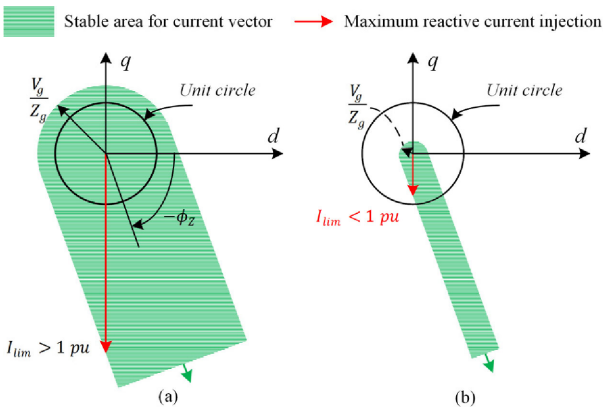

FIGURE 4. Depiction of the stable area of injected current vector during grid faults. (a) A grid fault where $V_g/Z_g > 1$pu, (b) A severe grid fault where $V_g/Z_g < 1$ pu and nominal capacitive reactive current cannot be injected as requested by the grid code. Both cases are shown for X/R = 2.5. I_{lim} denotes the maximum amount of reactive current provision from (2).

maximum static power transfer between its terminal bus and the grid. This limitation is present for any control structure (grid-following and grid-forming) and is a condition for the existence of equilibrium points in the system. Therefore, this limitation is a necessary stability condition, ensuring that the converter operation represents a stable operation point [7], [36]. Considering the grid-following converter in Fig. 1, the q-axis component of PCC voltage, which is used for grid-synchronization, can be expressed as

$$v_{PCCq} = V_g \sin(\theta_g - \theta_{PLL}) + I_{PCC} Z_g \sin(\theta_I + \varphi_Z) \quad (1)$$

where φ_Z is the angle of the grid impedance. For stable operation, the PLL must be able to control the q-axis voltage component to zero. It should be noticed that the second right-hand term behaves as a destabilizing positive feedback term in the PLL control since the PLL is only able to regulate the first term [27], [37]. Therefore, if the grid is weak (large Z_g) or during a severe fault where V_g is small, the PLL may not be able to control the q-axis voltage to zero, causing the synchronization instability. By setting $v_{PCCq} = 0$, the stability condition with an inequality can be formulated as

$$I_{PCC} < \frac{V_g}{|Z_g \sin(\theta_I + \varphi_Z)|}. \quad (2)$$

From (2), it is noted that only a limited current magnitude (I_{PCC}) can be injected, given a current injection angle, a grid impedance, and a grid voltage magnitude. For a fully active current injection ($\theta_I = 0$), the limit is reduced to the ratio between the grid voltage magnitude and the grid reactance. However, during severe grid faults where a fully reactive current provision is often required, the current injection limit reduces to the ratio between the grid voltage magnitude and the grid resistance. This is exemplified in Fig. 4 where the stable area highlighted is the region where the injected current vector satisfies the expression in (2). Here, it can be seen that the more severe the grid fault is, the more limited is the stable region. As shown in Fig. 4(b), the voltage may drop so low that the 1 p.u. reactive current provision cannot be achieved without overloading the converter by injecting additional active current. Further, during normal operations, it can be appreciated from (2) that the minimum short-circuit ratio (SCR) for an inductive grid is 1 p.u., considering the static power transfer limitation. It is important to note that the power flow direction also influences the stable operating area. As can be seen in Fig. 4, the stability limit is not only influenced by the direction of the active power flow, but is also highly affected by the direction and magnitude of the provided reactive power.

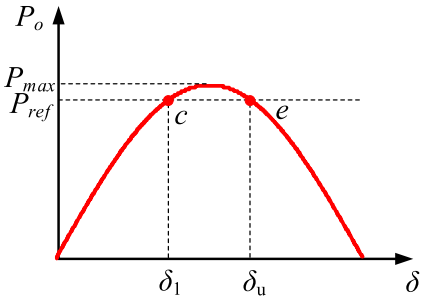

FIGURE 5. P_o-δ curve of grid-forming converters.

For grid-forming converters, its output active power can be calculated as

$$P_o = \frac{3}{2} \cdot \frac{V_o V_g \sin\delta}{X_g} \quad (3)$$

which can be visualized by the well-known P_o-δ curve, as given by Fig. 5, where point c and e are defined as the stable equilibrium point (SEP) and the unstable equilibrium point (UEP), respectively. The maximum active power that can be transferred from the grid-forming converter to the grid is defined as $P_{\max}$ in Fig. 5, and it is clear that $P_{ref} \leq P_{\max}$ is required for the existence of an equilibrium point.

III. GRID-FOLLOWING CONVERTERS

A. SMALL-SIGNAL SYNCHRONIZATION STABILITY

A conceptual explanation of the synchronization stability of grid-following converters in low SCR grids is given first. With a low SCR, the PCC voltage of the converter is severely affected by the current injected into the grid. The variation of the PCC voltage is then propagated through the PLL in Fig. 1, impacting the converter current. Thus, a self-synchronization loop is formed, which can deteriorate the synchronization stability of grid-following converters.

1) SIDEBAND OSCILLATIONS

In low SCR grids, the synchronization instability of grid-following converters can result in sideband oscillations in the voltage and current waveforms, whose waveforms are given in Fig. 6. From the spectrum of i_a, it is seen that the sideband oscillations around the grid fundamental frequency, i.e. $f_1 \pm f$ (88 Hz and 12 Hz), are generated, where f_1 is the fundamental frequency [14].

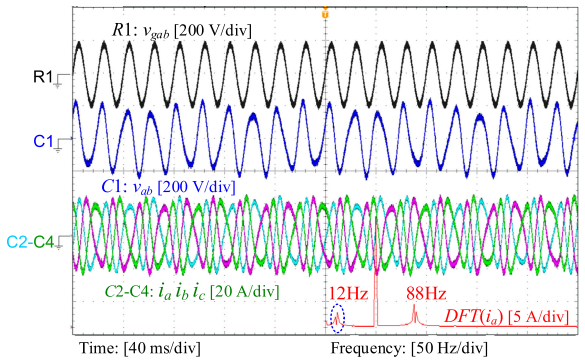

FIGURE 6. Sideband oscillations of grid-following converters when SCR is 2 [39].

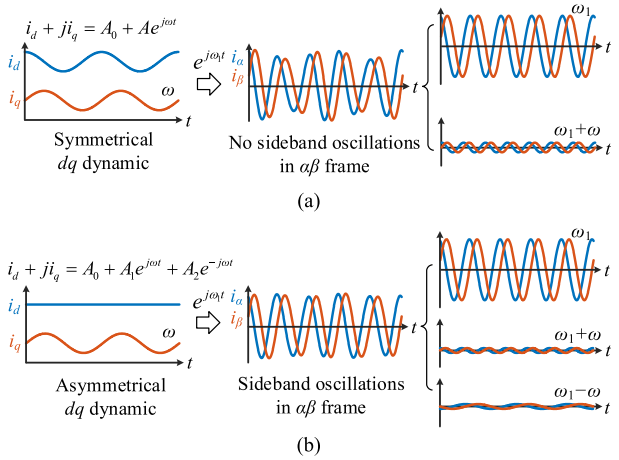

FIGURE 7. Sideband oscillation illustration. (a) Symmetrical dq-frame dynamic. (b) Asymmetrical dq-frame dynamic.

The sideband oscillation is induced by the asymmetrical control dynamics in the *dq*-reference frame [38], which can be illustrated by Fig. 7. If the converter only has symmetrical control loops, the *dq* frame oscillation at the frequency (ω) only results in a frequency-shifted response ($\omega_1 + \omega$) when transformed into the $\alpha\beta$ frame. However, the grid-following converters have asymmetrical control loops. For instance, the synchronization unit, i.e., PLL, only regulates the *q*-axis PCC voltage, as shown in Fig. 1(b). Consequently, the asymmetrical dynamics in the *dq* frame ($\pm\omega$) are inevitable, which propagate through the inverse Park transformation, resulting in sideband oscillations in the $\alpha\beta$ frame ($\omega_1 \pm \omega$).

2) SMALL-SIGNAL MODELING AND ANALYSIS

Small-signal modeling and stability analysis can characterize the sideband oscillations induced by the PLL of grid-following converters in low SCR grids. To briefly illustrate the negative damping mechanism of the PLL, a simplified small-signal model based on the feedback control loop of θ_{PLL} can be derived, as shown in Fig. 8. The control dynamics are modeled in the *dq*-reference frame, where the impacts of CC, DVC, and AVC are neglected. It can be seen that the PLL itself forms a negative feedback control loop, as shown in the grey

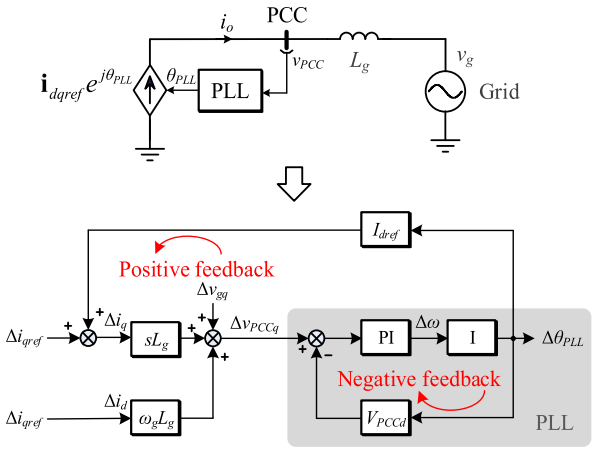

FIGURE 8. Simplified small-signal model of synchronization control loop considering the PLL and grid dynamics.

box. Additionally, the interaction with the grid impedance leads to a positive feedback control loop when $I_{dref} > 0$ (i.e., the inverter mode). The PLL is in cascade with the positive feedback control loop, and hence, adversely affects the synchronization stability of grid-following converters. More specifically, with higher values of I_{dref} and L_g, corresponding to a lower SCR, the gain of the positive feedback control loop is increased. With a higher control bandwidth of the PLL, the effective frequency range for the positive feedback control loop with a high gain is widened. Therefore, both the high PLL bandwidth and the low SCR of the grid can deteriorate the synchronization stability of grid-following converters [40].

The eigenvalue-based analysis and the impedance-based analysis are two common approaches to analyze the synchronization stability of grid-connected converters. The eigenvalue-based analysis relies on building an explicit state-space model of the entire system, then the sensitivity analysis of PLL control parameters can reveal its negative damping to the oscillation modes [41].

The impedance-based analysis is more suitable to analyze so-called "black-box" systems. The converter-grid interaction can be modeled by equivalent impedances seen from the PCC. Such impedance models form an open-loop gain of the system, where subsequently the stability is evaluated using the Nyquist stability criterion [42]. The impedance-based analysis enables us to provide physical insight into the converter-grid interaction from the passivity perspective [38]. The negative damping contributed by the PLL has been interpreted as a negative resistance (non-passive) in the low-frequency range, which jeopardizes the converter-grid stability [27], [43]. It is noted that due to the asymmetrical *dq*-frame dynamics induced by the PLL, the converter impedance model has to be characterized as a multi-input multi-output (MIMO) matrix. Thus, the passivity needs to be evaluated through the passivity index [38]. To simplify the MIMO-based analysis, two equivalent single-input single-output (SISO) impedance ratios are derived from a closed-loop MIMO model

TABLE 1. Stabilizing Methods for Small-Signal Stability Enhancement of Grid-Following Converters in Weak Grids

Stabilizing methods	Proposals
Controller tuning	• Reducing PLL bandwidth [46]
Modifications on PLL	• Damping controller in PLL [47] • Virtual impedance embedded in PLL [48] • Symmetrical PLL for SISO-based impedance shaping [39]
Feedforward-based control	• Virtual impedance [47], [49], [50] • Feedforward control from the PLL [51]
Grid-forming control	• Replace grid-following control with grid-forming control [52]

including the grid impedance [44], [45]. Thus, the synchronization stability can be evaluated by using the SISO impedance-based analysis [42]. Yet, the equivalent SISO impedances of converters are composed by impedance terms of converter and grid, which fails to shed clear insight into the passivity of converter impedance.

3) STABILIZING CONTROL: CONTROLLER TUNING AND ADDITIONAL DAMPING

Many research efforts have been made to mitigate the sideband oscillations of grid-following converters operating in low SCR grids, which are summarized in Table 1. The most common practice is to tune the PLL control parameters. According to Fig. 8, since the PLL works like a LPF, by reducing its control bandwidth, the effective frequency range of the positive feedback loop is reduced, such that the synchronization stability can be improved. It is also found that reducing the PLL bandwidth also results in a reduced frequency range of the negative resistance in the converter output impedance, which explains the stability enhancement from the passivity perspective [46].

In addition to the controller tuning, several active damping control methods have been reported to improve the dynamic performance of grid-following converters in low SCR grids. Since the PLL is the root cause that destabilizes the system, some efforts are directly put on the modifications of the PLL, whose control diagrams are summarized in Fig. 9.

A damping controller with a band-pass filter (BPF) is proposed in [47], where the negative resistance caused by the PLL can be minimized by tuning the BPF. In [48], a virtual impedance is embedded with the PLL, such that the VSC is synchronized with a remote stronger voltage behind the virtual impedance. The negative impact of grid impedance on the synchronization stability can thus be reduced. The two methods directly apply active damping by modifying the PLL, yet the controller tuning depends on the grid condition. A symmetrical PLL is further proposed in [39], which establishes a pair of complex phase angles ($\theta_{PLLd} + j\theta_{PLLq}$) through the symmetrical control dynamics. Although the PLL itself is not intended for active damping, its symmetrical structure enables a SISO-based impedance shaping for stability enhancement.

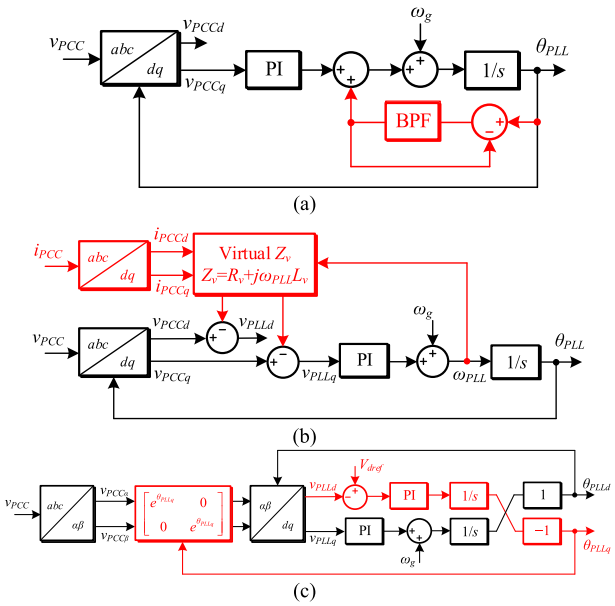

FIGURE 9. Modification schemes based on PLL for stabilizing. (a) BPF-based active damping within PLL [47]. (b) Virtual impedance embedded with PLL [48]. (c) Symmetrical PLL for SISO-based impedance shaping [39].

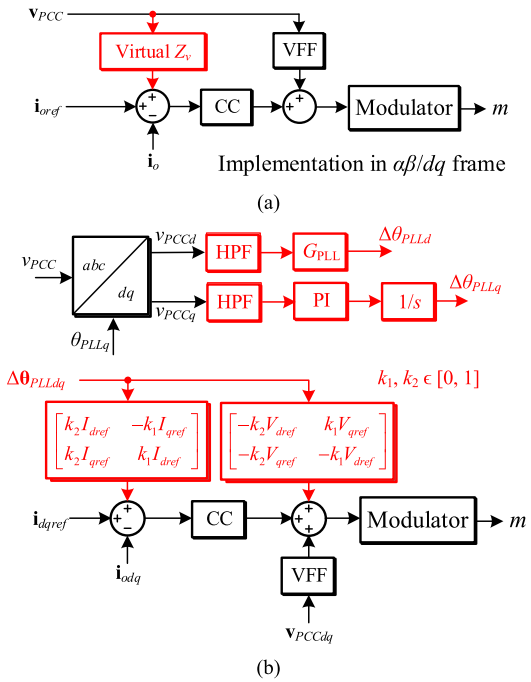

FIGURE 10. Feedforward-based control for stabilizing. (a) Virtual impedance [47], [49]. (b) Feedforward from PLL [51].

Besides modifying the PLL, the feedforward-based control is also commonly used for active damping. One general approach is based on the virtual impedance control, where a feedforward control loop from the PCC voltage can be added to the current reference, to realize impedance shaping and reduce the negative resistance caused by the PLL [47], [49], as shown in Fig. 10(a). It is noted that the control implementation

of the virtual impedance can be flexible in either the $\alpha\beta$ or dq frame. Also, the voltage feedforward control can be alternatively added to the modulation voltage [50], which results in a similar damping effect. These virtual impedance control designs still rely on the grid condition, thus a parameter tuning effort is needed. Alternatively, a recent work reported in [51] designs a feedforward loop from the PLL to the current control, based on establishing symmetrical dynamics in d and q axes, whose control diagram is given in Fig. 10(b). This method mitigates the frequency couplings caused by the PLL, which contributes to the synchronization stability in low-SCR grids.

The above stabilizing methods mainly tackle the negative damping caused by the PLL. In recent years, some studies have revealed that the grid-forming control achieves superior stability in weak grids compared to the grid-following control [52], since the PLL is not needed for grid-forming control, and thus the corresponding positive feedback control loop can be avoided. However, the grid-forming control introduces other challenges for synchronization stability, which will be further discussed in Section IV.

B. LARGE-SIGNAL SYNCHRONIZATION STABILITY

Besides the synchronization stability in low SCR grids, large-signal synchronization (transient) instability is a large threat to the power system security during grid faults and large load-generation imbalances. In the following, the loss of synchronization (LOS) phenomenon during grid faults is visualized first. The large-signal dynamic model for transient stability is then discussed, which is followed by a design-oriented analysis and countermeasures by control to enhance the transient stability.

1) LOSS OF SYNCHRONIZATION PHENOMENON

The transient instability may occur for two reasons: i) the necessary stability condition in (2) is violated, i.e. a stable operating point does not exist during the fault, and ii) the synchronization dynamics do not possess sufficient damping to be attracted to the stable operation point during the fault. Fig. 11 shows experimental waveforms of LOS caused by the insufficient damping during a severe symmetrical grid fault, although, the necessary stability condition given in (2) is satisfied. As can be seen, the injected currents seen from the PLL rotating frame are following the current references, prioritizing reactive current support during the fault. However, when referring the injected currents to the actual phase-angle of the PCC voltage, large low-frequency oscillations are observed, which distorts the PCC voltage towards a voltage collapse.

2) LARGE-SIGNAL MODELING

For the transient stability assessment, the PLL-synchronized grid-following converter can be represented as a second-order nonlinear equation as [53]

$$0 = \ddot{\delta} + D(\delta)\dot{\delta} + F(\delta, \dot{\delta}) \tag{4}$$

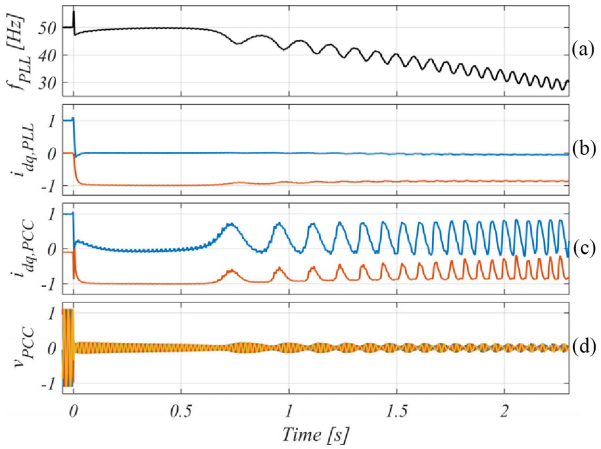

FIGURE 11. Experimental waveforms, visualizing loss of synchronization during a severe symmetrical grid fault where the grid voltage drops to 0.045 pu. (a) Unstable PLL frequency estimation. (b) DQ-axes currents relative to the PLL phase angle. (c) DQ-axes currents relative to the actual phase angle of the PCC voltage. and (d) Three-phase faulted voltage at the PCC [53].

where

$$D(\delta) = \frac{K_{pPLL} V_g \cos(\delta)}{1 - K_{pPLL} I_{PCC} L_g \cos(\theta_I)}, \tag{5}$$

$$F(\delta, \dot{\delta}) = \frac{K_{iPLL}[V_g \sin(\delta) - Z_g(\dot{\delta}) I_{PCC} \sin(\theta_I + \varphi_g(\dot{\delta}))]}{1 - K_{pPLL} I_{PCC} L_g \cos(\theta_I)}, \tag{6}$$

$\delta = \theta_g - \theta_{PLL}$, and the grid impedance magnitude and phase are based on the real-time PLL frequency. For the model in (4), the converter is represented as an ideal controllable current source, which is oriented by the output phase of the PLL. Such an approximation is justified by the fact that the timescale of PLL-induced LOS is much slower than that of the inner current control [53], [54].

Since the model in (4) is second-order and nonlinear, no known analytical solution exists. Therefore, to assess the stability, either an approximation of the model has to be made or it has to be computed using numerical integration. In [55], [56], it is revealed that the second-order nonlinear model in (4) can be further rearranged to the same form as the power-angle swing equation of a synchronous machine, which is given by

$$\underbrace{\frac{1 - K_{pPLL} I_{PCC} L_g \cos(\theta_I)}{K_{iPLL}}}_{\text{Equivalent moment of inertia}} \ddot{\delta} = \underbrace{Z_g(\dot{\delta}) I_{PCC} \sin(\theta_I + \varphi_g(\dot{\delta}))}_{v_{zq}} - \underbrace{V_g \sin(\delta)}_{v_{gq}} - \dot{\delta} \underbrace{\frac{K_{pPLL}}{K_{iPLL}} V_g \cos(\delta)}_{\text{Damping}}, \tag{7}$$

where v_{zq} and v_{gq} are the q-axis components of the voltage across the line impedance and the grid voltage, respectively. Eq. (7) forms the nonlinear voltage-angle "swing" equation, where the virtual moment of inertia is inversely proportional

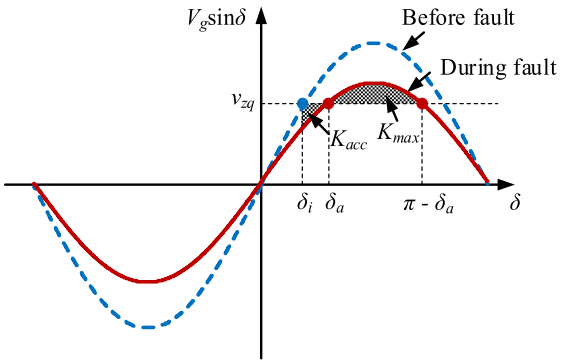

FIGURE 12. Nonlinear voltage angle curve shown for a pre-fault condition and during a fault. The q-axis voltage terms can be interpreted as equivalent mechanical and electrical power. The accelerating area (K_{acc}) and maximum allowed decelerating area (K_{max}) is used in the EAC formulation to assess the transient stability of the system.

to the PLL integral gain, and the system damping is proportional to the ratio between the PLL controller gains. It is evident that the transient stability can be enhanced by increasing the proportional gain or decreasing the integral gain of the PLL. With this analogy to the synchronous machine swing equation, analytical assessment methods employed in the field of synchronous generation can be used for grid-following converters. Fig. 12 shows the voltage-angle curve of grid-following converters, where the equal-area criterion (EAC) is adopted in [7], [56] to assess the transient stability of the system. With the EAC, the decelerating and accelerating areas depicted in Fig. 12 can be analytically determined and instability is concluded when $K_{acc} > K_{\max}$ [7]. However, the system damping is neglected in the EAC formulation, which is achieved by setting the PLL proportional gain to zero. This approximation is, however, not realistic in a practical design of the PLL [43], which causes the EAC to be conservative in its assessment.

Besides the EAC criterion, the Lyapunov theory has also been used to assess the transient stability of the system. In [57], the grid-following converter is modeled as an electrostatic machine where the Popov method is used to find a Lyapunov function to assess the large-signal stability of the system. This method also assumes a damping-less system, which gives a conservative stability assessment. In [58], a catastrophic bifurcation phenomenon is identified for grid-following converters under grid fault conditions. Here, it is observed that the converter cannot synchronize with the grid and that voltage saturation limit imposed by the available dc-link voltage causes a structural change to the system during saturation, which causes instability that cannot be restored after fault recovery. Using the above direct methods, the damping ratio is overlooked, which is infeasible for PLL-synchronized converters. Hence, a design-oriented analysis considering the damping effect of the PLL is needed.

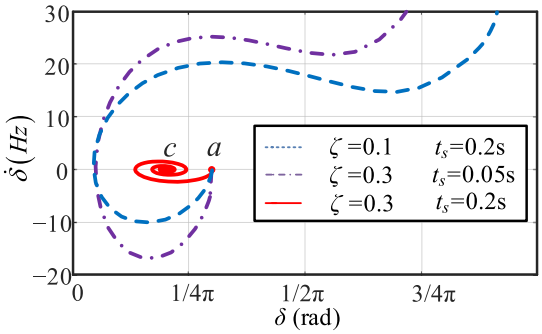

FIGURE 13. Phase portraits of the PLL when V_g drops from 1 p.u. to 0.6 p.u. $\zeta = 0.3$, $t_s = 0.05$s (unstable), $\zeta = 0.1$, $t_s = 0.2$s (unstable), $\zeta = 0.3$, $t_s = 0.2$s (stable) [22].

3) DESIGN-ORIENTED ANALYSIS OF TRANSIENT STABILITY

As mentioned above, the impact of controller parameters of the PLL needs to be considered for the accurate transient stability assessment. The damping ratio (ζ) and the settling time (t_s) of the PLL are defined as

$$\zeta = \frac{K_{pPLL}}{2}\sqrt{\frac{V_g}{K_{iPLL}}} \tag{8}$$

$$t_s = \frac{9.2}{V_g K_{pPLL}} \tag{9}$$

For the second-order nonlinear differential equation given by (4), the phase portrait can be adopted for obtaining a graphical solution, which is intuitive and facilitates the design-oriented analysis.

Fig. 13 shows the phase portraits of a grid-following converter with different ζ and t_s. Points a and c represent the system's SEPs before and after the fault, respectively. The system is stable when the phase portrait converges to the SEP c after the fault and is unstable when the phase portrait diverges. From Fig. 13, it is clear that the transient stability of grid-following converters can be enhanced by increasing the ζ and t_s of the PLL.

Using phase portraits, the critical system damping and area of attraction of the nonlinear system can be estimated by sweeping a set of initial conditions for PLL controller gains [59]. This is exemplified in Fig. 14, where the PLL integral gain is swept from the initially designed value to a lower value, which provides higher damping and, therefore, enhanced transient stability. As can be noticed in Fig. 14, for a decreasing fault voltage magnitude, the critical PLL damping needs to be significantly increased for the phase trajectory to be attracted to the stable operating point during the fault.

4) STABILIZING CONTROL

There are, in general, two categories of control methods for enhancing the transient stability of grid-following converters. *a) Modified Active Current or Active Power:* The first category of control methods is to modify the injected active current during the fault. These methods are listed in Table 2.

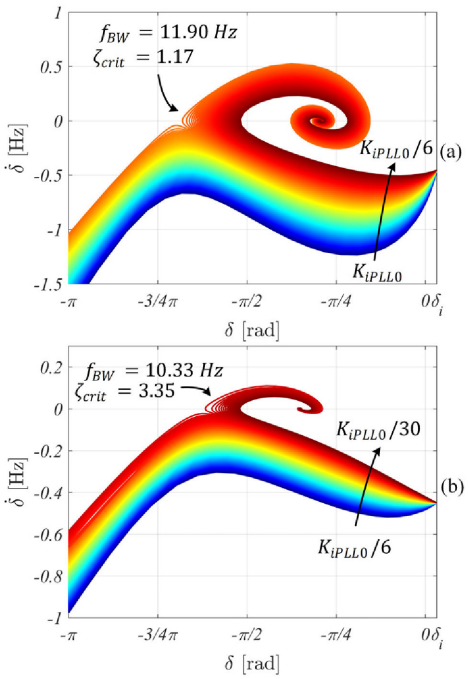

FIGURE 14. Phase portraits for varying K_{iPLL} during a severe symmetrical fault where the critical damping and area of attraction can be extracted. The grid voltage magnitude during the fault drops to (a): $V_g = 0.05$ *pu*, (b): $V_g = 0.045$ *pu*. The grid impedance is $Z_g = 0.04 + 0.1j\ \Omega$ and K_{iPLL0} denotes the initial design for the PLL integral gain. Each subplot contains 200 different initial conditions used to estimate the area of attraction [59].

TABLE 2. Stabilizing Control to Mitigate Transient Instability Based on Changing the Injected Current Vector

Ref.	Proposal
[60]	Reduced active current proportional to voltage drop during fault
[36]	Increase active current reference based on the PLL frequency error
[61]	Increase active power reference based on the PLL frequency error
[62]	Align current vector angle with line impedance angle
[63]	Set reference power equal to actual power to eliminate ac-/de-celerating areas in EAC

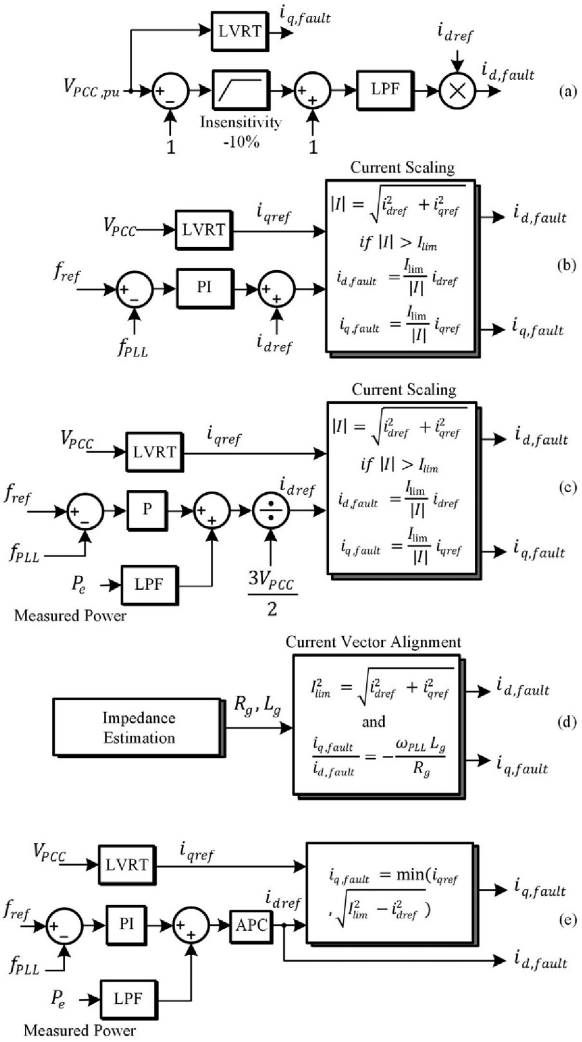

FIGURE 15. Stabilizing control through modifying the active current component during the fault. (a) Active current reduction based on voltage drop [60]. (b) Active current injection based on PLL frequency error [36]. (c) Active power injection based on PLL frequency error [61]. (d) Alignment of the current vector into a stable operating area [62]. (e) Cancellation of ac-/de-celerating areas in EAC and damping provision [63].

In addition to these, it is also proposed to reduce or cancel the current injection to improve stability during severe faults [64]. However, these methods do not comply with the grid codes and are, therefore, not included here. The block diagrams of the proposed methods from Table 2 are shown in Fig. 15. During faults where the reactive current is limited to 1 pu and the converter possesses short-term overloading capability, providing room for injecting active current, instability may occur as the active current component pushes the current vector into an unstable operating area [60]. To address this issue, it is proposed in Fig. 15(a) to reduce the active current in proportional to the experienced voltage drop during the fault. This method has a straight-forward implementation but suffers from the fact that the active current during the fault is low in many applications, and a pure reactive current cannot be injected. In such cases, it is desired to increase the active current rather than decreasing it. This is considered in Fig. 15(b), where the active current is increased based on the PLL frequency error. This method, as proposed in [36], contains a closed-loop controller where the PLL frequency signal is used as a feedback to detect LOS and regulate the active current, such that the injected current vector moves to a stable operating area. This method has the advantage that it can address the problems with either too low or too high active current during the fault. However, it introduces an additional closed-loop control where its stability is not discussed or proven.

A similar approach is proposed in Fig. 15(c), where the active power reference is modified instead of the active current. From (2), it can be seen that if the injected current vector is aligned with the negative grid impedance angle, a stable operating point will always result [62]. This fact is utilized in

TABLE 3. Stabilizing Control to Mitigate Transient Instability Based on Modifying the Synchronization Dynamics

Ref.	Proposal
[66], [67]	Freeze the PLL during the fault
[59], [68]	Increase damping ratio of PLL
[69]	Gain schedules K_{iPLL} during fault
[22], [70]	Switch PLL to a first-order loop during fault

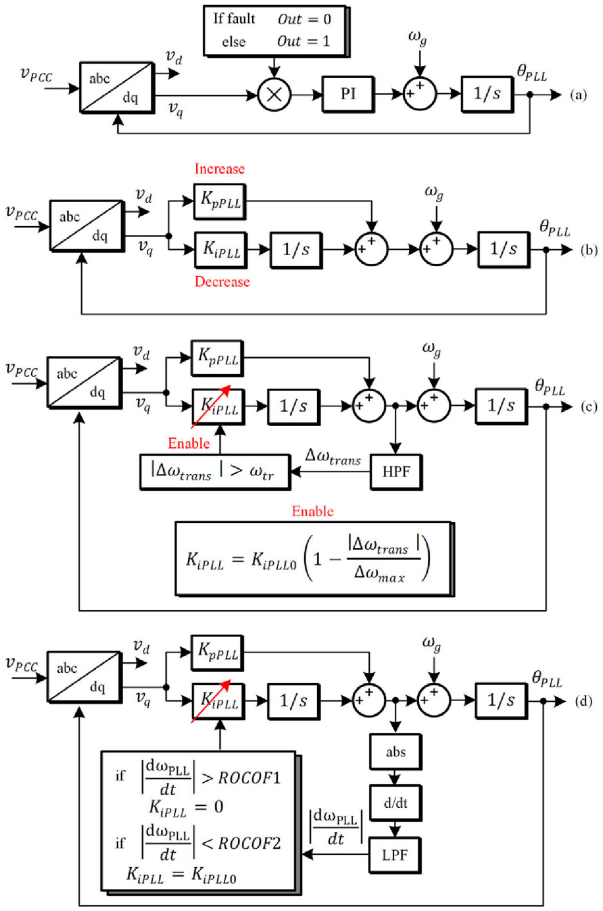

FIGURE 16. Stabilizing control through modifying the PLL synchronization dynamics during the fault. (a) PLL freezing method [66], [67]. (b) Increase PLL damping ratio [59], [68]. (c) Gain schedules the PLL integral gain depending on estimation frequency change [69]. K_{iPLL0} is the initial designed integral gain. (d) Switch to a first-order PLL when maximum ROCOF is exceeded [22], [70].

the proposal in Fig. 15(d), where the injected current vector is aligned in this way. This method has the advantage of always proving a stable operation and its transient stability can be mathematically proven. However, this method needs a rapid estimation of the impedance angle when the fault occurs. In [65], such an estimation of impedance angle is reported, which can be utilized with the control scheme in Fig. 15(d) for stability enhancement. Lastly, another approach similar to those discussed in [38], [64] is proposed in Fig. 15(e) [63]. Here, the stabilizing idea is based on the principles of the EAC. If the reference power is set equal to the measured active power ($P_m = P_e$), then ideally, the accelerating and decelerating areas are eliminated, which means that stability can be achieved with any positive damping term. However, as shown in (7), the damping is a nonlinear function of δ and can, therefore, not be guaranteed positive. To address this issue, Fig. 15(e) uses a PI controller on the PLL frequency error. With this, it is shown that the proportional gain of this controller introduces additional damping, which can be designed to always compensate for potential negative damping in (7).

b) Modified PLL Parameters: The second branch of stabilizing control methods modify the PLL parameters to enhance the transient stability. These are listed in Table 3 and their proposed control structures are depicted in Fig. 16. The simplest method is the PLL freezing method visualized in Fig. 16(a), which nullifies the PLL control error when a predefined severe fault is detected [66], [67]. This effectively makes the PLL-synchronized converter able to operate in a stand-alone mode based on its pre-fault frequency and phase estimations. This method has the advantage that it allows the converter to operate under any condition, including zero-voltage conditions, and will always operate at a stable operating point, no matter the fault severity. As this method freezes its internal states, it is unaware of phase-angle jumps and frequency drifts during the fault. In the second method in Fig. 16(b), the proportional gain and integral gain of the PLL are increased and decreased, respectively, to improve the system damping, which enhances the transient stability. This method is simple to implement, yet it only works when the converter has two equilibrium points during the fault and lacks parameter-tuning guidelines. The third method ([59], [68]) shown in Fig. 16(c), proposes gain scheduling of the PLL integral gain based on the transient dynamics in the estimated PLL frequency. This effectively decreases the integral gain towards zero if instability occurs. $\Delta\omega_{\max}$ is the maximum frequency band around nominal considered, here 10 Hz. Compared to the method in Fig. 16(b), this has the advantage of increasing the PLL damping sufficiently during transients without having to select a pre-defined specific value. Nevertheless, it suffers from not being able to address faults where only one equilibrium point exists during the fault or in cases where the two operating points are very close to the necessary stability condition. In either case, the overshoot from the second-order dynamics may still cause instability. This issue is addressed in [22], [70], Fig. 16(d), where the PLL is switched to a first-order loop during the fault, eliminating the integral gain. The activation of the first-order loop is based on a rate-of-change-of-frequency (ROCOF) threshold rather than a fault signal based on the voltage magnitude. Hence, if instability does not occur, the proposed method will not remove the integral gain. The proper selection of the ROCOF values is discussed in detail in [22]. This method has the advantage that it can stabilize any system with a least one operating point.

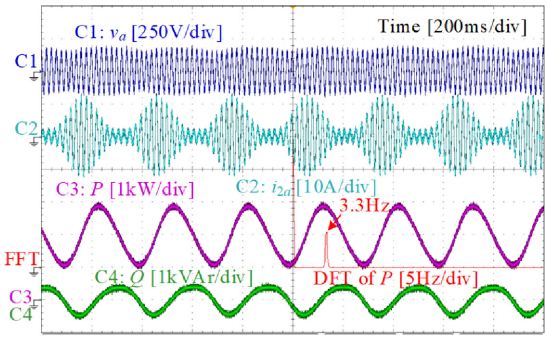

FIGURE 17. Sideband oscillations of grid-forming converters when SCR is 10 p.u. [17].

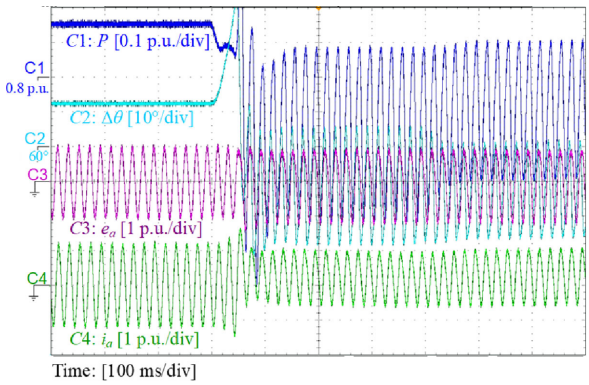

FIGURE 18. Synchronous oscillations of grid-forming converters [71].

During a severe fault, where no operating points exist, one still needs to switch to, e.g., a PLL freezing method or some of the methods presented in Fig. 15 to remain stable.

IV. GRID-FORMING CONVERTERS

A. SMALL-SIGNAL SYNCHRONIZATION STABILITY

Differing from grid-following converters, the grid-forming converter may suffer from small-signal instability in stiff grids [16]. Since grid-forming converters regulate their PCC voltages directly, the voltage regulation tends to be more difficult if two voltage sources are electrically close to each other. There are two types of synchronization instability phenomena for grid-forming converters: 1) sideband oscillations and 2) synchronous oscillations.

1) SIDEBAND OSCILLATIONS

The first type of instability is the sideband oscillation of the grid fundamental frequency, similar to that of grid-following converters in low SCR grids. This phenomenon is due to the asymmetrical dynamics of grid-forming converters in their outer-loop power control.

Fig. 17 shows experimental waveforms for grid-forming converters operating in stiff grids. The sideband oscillations can also be observed in the voltage and current waveforms, which turn into low-frequency oscillations in the power waveforms.

Several studies have been reported recently to characterize the sideband oscillations. It has been found that the inner-loop voltage control of grid-forming converters also plays a vital role in the negative damping [17]. It is also revealed that the voltage feedback decoupling loop added at the output of the innermost current control loop has a detrimental impact on the stability of grid-forming converters in stiff grids [18]. Besides, the power control parameters, e.g., the droop control coefficient [19], the converter operating point [20], and the line dynamics [16], also impact the sideband oscillations.

In addition to stiff-grid scenarios, grid-forming converters can also induce sideband oscillations in series-compensated weak grids [21]. In such cases, the grid impedance has an abrupt change from inductive to capacitive behavior near the fundamental frequency, which tends to interact significantly with the grid-forming converter and lead to the sideband oscillations. It is found that the stability becomes worse as the series compensation level increases since the resonant frequency of the grid impedance moves towards the grid fundament frequency.

2) SYNCHRONOUS OSCILLATIONS

The second type of small-signal synchronization instability of grid-forming converters is the synchronous oscillation [10]. Fig. 18 shows the measured synchronous oscillation waveforms of grid-forming converters with a step change of active power reference, where oscillations at the fundamental frequency appear in the power waveform (C1), corresponding to the second-order harmonics and dc offsets in the voltage and current waveforms (C3 and C4). This is in principle induced by the power transfer through electrical networks. The small-signal model of the plant in the power synchronization control loop can be derived as [72]

$$\begin{bmatrix} P(s) \\ Q(s) \end{bmatrix} = \begin{bmatrix} G_{P\delta}(s) & G_{PV}(s) \\ G_{Q\delta}(s) & G_{QV}(s) \end{bmatrix} \begin{bmatrix} \delta(s) \\ V(s) \end{bmatrix}$$

$$\text{where } G_{P\delta}(s) = \frac{\omega_g L_g V_0 V_g \cos\delta_0 - (sL_g + R_g) V_0 V_g \sin\delta_0}{(sL_g + R_g)^2 + (\omega_g L_g)^2}$$

$$G_{PV}(s) = \frac{(sL_g + R_g) V_0 \cos\delta_0 + \omega_g L_g V_0 \sin\delta_0}{(sL_g + R_g)^2 + (\omega_g L_g)^2}$$

$$G_{Q\delta}(s) = -\frac{(sL_g + R_g) V_0 V_g \cos\delta_0 + \omega_g L_g V_0 V_g \sin\delta_0}{(sL_g + R_g)^2 + (\omega_g L_g)^2}$$

$$G_{QV}(s) = \frac{\omega_g L_g V_0 \cos\delta_0 - (sL_g + R_g) V_0 \sin\delta_0}{(sL_g + R_g)^2 + (\omega_g L_g)^2} \quad (10)$$

It is seen that the inductive line parameters result in a synchronous resonance peak in the plant models, and the line resistance adds damping to the synchronous resonance. Therefore, such an issue is more severe in systems with low

TABLE 4. Stabilizing Methods for Small-Signal Stability Enhancement of Grid-Forming Converters

Issues	Stabilizing methods
Sideband oscillations	• Reducing power-loop controller gains [19] • Reducing voltage feedback decoupling gain [18] • Multi-loop damping controllers in APC [74], [75] • Lead-lag compensation in APC and RPC [76] • Active power feedforward [76] or frequency dependent voltage control [77], [78] • Virtual impedance control for series-compensated grids [21]
Synchronous oscillations	• Increasing virtual inertia (reducing power control bandwidth) [73] • Virtual impedance control [10] • Phase compensation in power loop [72] • Cross-coupling control schemes [71], [72]

R/X ratios. The synchronous resonance was overlooked in conventional synchronous generators, due to the slow electromechanical dynamics [73]. However, it becomes more evident in grid-forming converters, since the power is controlled much faster.

3) STABILIZING CONTROL: CONTROLLER TUNING AND ADDITIONAL DAMPING

Stabilizing control methods have been developed to address the sideband oscillations and the synchronous oscillations of grid-forming converters, which are summarized in Table 4. The sideband oscillations can be mitigated by tuning the control parameters, such as reducing the power-loop controller gains [19], or reducing the voltage feedback decoupling gain [18].

Some additional damping control schemes of sideband oscillations are developed for grid-forming converters, whose diagrams are provided in Fig. 19. Multi-loop controllers can be embedded into the APC to dampen the low-frequency oscillations in the power waveforms [74], as shown in Fig. 19(a), where the center frequencies (ω_n) of the BPFs are tuned at the oscillation modes and the LPFs are used to emulate swing equations. The oscillation modes can be predicted by artificial intelligence [75]. This method is simply designed within the APC loop. Another method applies lead-lag compensators (G_{llp} and G_{llq}) in both the APC and RPC loops [76], as shown in Fig. 19(b). Similar to the previous one, the design of the lead-lag compensators relies on the oscillation modes. In addition, since the compensators are in cascade within APC and RPC loops, they may affect the power control bandwidth. Alternatively, the active power feedforward control [76] or the frequency dependent voltage control [77], [78] can be applied for stabilizing the system. However, those controllers strengthens the dynamic couplings between the APC and RPC, and their design are dependent on grid conditions [76]. In addition to the shaping of power control loops, the virtual impedance-based control can be designed with the inner loop dynamics, whose principle in active damping is similar to

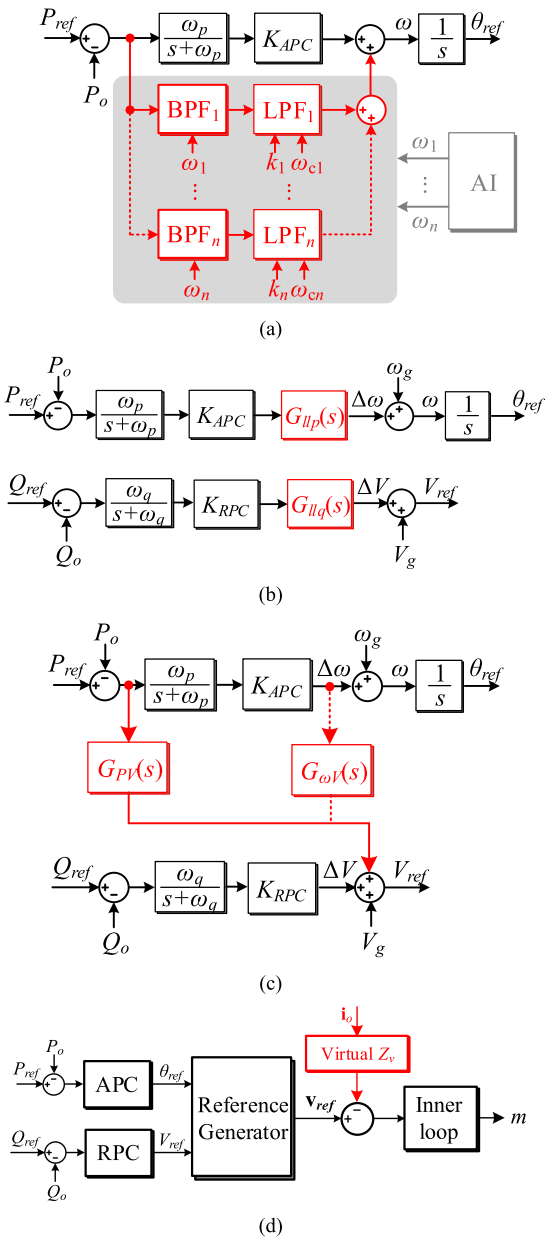

FIGURE 19. Stabilizing control schemes for sideband oscillation damping. (a) Multi-loop controllers in APC [74] with artificial intelligence [75]. (b) Lead-lag compensation in power loop [76]. (c) Active power feedforward [76] or frequency dependent voltage control [77], [78]. (d) Virtual impedance control [21], [76].

that for grid-following converters [79]. This concept has also been applied to dampen the sideband oscillations in a series-compensated grid, where a current feedforward control that is directly added to the modulation voltage [21].

For the synchronous resonances, it can also be damped by controller tuning. With larger virtual inertia, a mechanical damping can be emulated to damp the resonance [73]. However, the method adds a low-pass filter in the APC, which sacrifices the power control bandwidth. Some additional damping approaches have been reported, as shown in Fig. 20. An easy

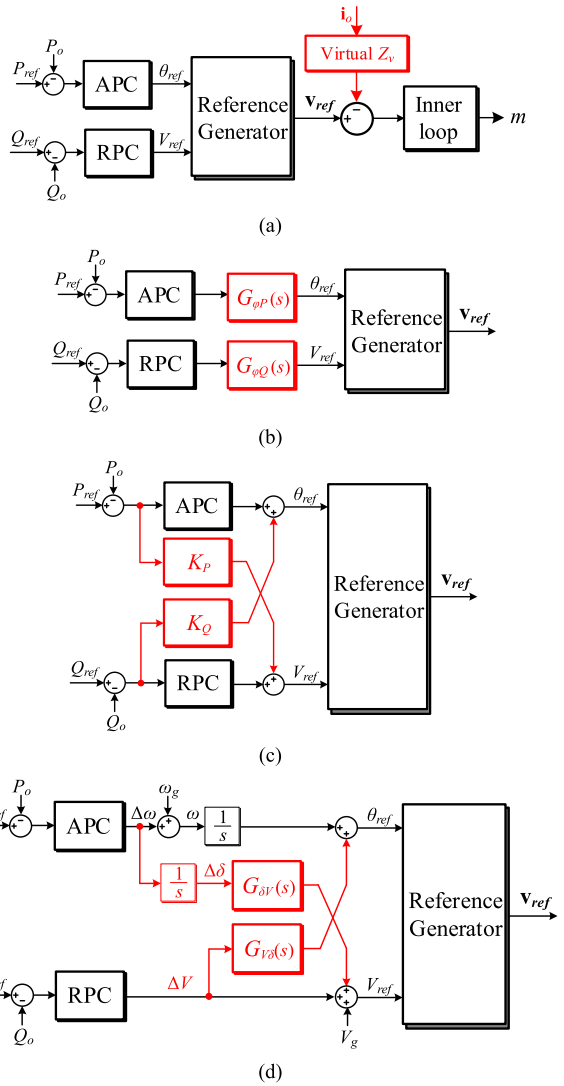

FIGURE 20. Stabilizing control schemes for synchronous oscillation damping. (a) Virtual impedance [10]. (b) Phase compensation filter [72]. (c) Cross feedforward compensation [72]. (d) Phase-amplitude cross regulation [71].

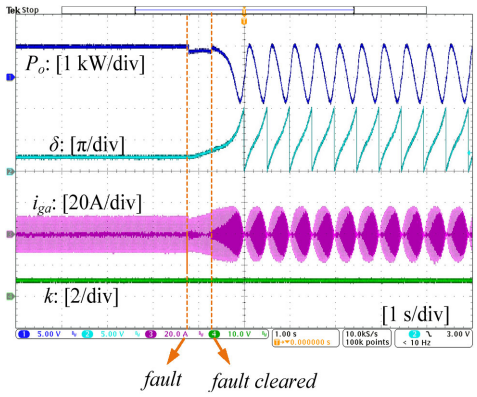

FIGURE 21. Experimental results of grid-forming converters after the fault clearance [80].

way is to implement the virtual impedance control [10], which emulates electrical damping in series with the line impedance in (10). This approach is in principle the same as Fig. 19(d) for the sideband oscillation suppression. Alternatively, the phase compensation filter can be directly deployed in the power loop [72], which avoids the phase crossing 180° at the synchronous resonant peak, thus contributes to the stability. The aforementioned two damping approaches can be simply designed based on the single APC or RPC loop, which are thus unable to address the cross-couplings in (10). Such cross-couplings can intensify the power oscillations between the two control loops [73]. A cross feedforward compensation method is thus utilized in [72], where two proportional damping terms are tuned to suppress the cross-couplings. Although the synchronous resonances can be mitigated more effectively with larger damping terms, the instability risk still exists since the cross-couplings cannot be fully compensated by the proportional damping terms. A phase-amplitude cross-regulation method is further proposed in [71], which not only fully eliminates the synchronous resonance, but also remarkably reduces the couplings between the APC and RPC. However, this decoupling control is merely designed assuming that $\delta_0 \approx 0$ in (10), which means that the steady-state phase angle difference between the converter PCC voltage and the grid voltage is negligible.

B. LARGE-SIGNAL SYNCHRONIZATION STABILITY

1) PHENOMENON

Similar to the large-signal synchronization stability issues of grid-following converters presented in Section III.B, the grid-forming converters may also lose synchronization with the power grid when subjected to large disturbances. The root causes of the LOS are:

- Lack of equilibrium points when P_{ref} is larger than the maximum power that can be transferred from the grid-forming converter to the grid (P_{max} in Fig. 5).
- The crossover of the UEP (point e in Fig. 5) due to the overshoot in the dynamic responses. Since $P_{ref} > P_o$ always holds after the UEP, the APC will continuously increase the output frequency of the grid-forming converters, and finally leads to the LOS.

Fig. 21 shows the measured waveforms for grid-forming converters with LOS after a fault clearance [80]. In this test, the equilibrium points of grid-forming converter are restored by clearing the fault. Although the controller parameters are tuned to assure the small-signal stability, the grid-forming converter still loses the synchronism with the power grid, due to the crossover of the UEP.

2) LARGE-SIGNAL MODELING AND ANALYSIS METHODS

The large-signal dynamics of grid-forming converters are determined by the APC and RPC loops, whose nonlinear

differential equations can be derived based on Fig. 3(c)

$$\ddot{\delta} = -\omega_p \dot{\delta} + \omega_p K_{pAPC}\left(P_{ref} - \frac{3}{2}\cdot\frac{V_o V_g \sin\delta}{X_g}\right) \tag{11}$$

$$\dot{V}_o = \omega_q\left(V_g - V_o\right) + \omega_q K_{RPC}\left(Q_{ref} - \frac{3}{2}\cdot\frac{V_o^2 - V_o V_g\cos\delta}{X_g}\right) \tag{12}$$

where ω_p and ω_q are cutoff frequencies of LPFs in the APC and RPC, respectively. It is difficult to obtain analytical solutions of (11) and (12) due to their nonlinearity. As an alternative, Lyapunov's direct method can be adopted for the transient stability assessment. Yet, it requires the derivation of a candidate Lyapunov function, which is challenging to obtain in practice [81]. In contrast, phase portraits that provides a graphical solution of first- and second-order nonlinear systems, are more intuitive and can be readily implemented.

a) First-Order Power Angle Control: In this part, the transient stability of grid-forming converters with the first-order power control, i.e., PSC or the basic droop control, will be analyzed. For simplicity, the dynamics of the RPC are neglected at first by assuming a constant V_o. Thus, the power angle dynamics can be simplified as [23]

$$\dot{\delta} = K_{APC}\left(P_{ref} - \frac{3V_oV_g}{2X_g}\sin\delta\right). \tag{13}$$

Based on (13), the phase portrait of grid-forming converters with the first-order power control can be plotted, as shown in Fig. 22(a). Due to the overdamped response brought by the first-order control dynamics, the grid-forming converter can always be stabilized at the SEP when there are equilibrium points during the disturbance, as shown in Fig. 22(a). Hence, the risk of crossing over the UEP is fully prevented by the first-order power control, which yields an attractive transient stability performance [23].

Moreover, in the case that there is no equilibrium point during the fault, the critical clearing angle (CCA) is fixed as δ_u, which is the power angle corresponding to the UEP, as shown in Fig. 22(b). Differing from the SG, where the LOS is inevitable if the fault clearing angle (FCA) is larger than CCA, the grid-forming converter with the first-order power control can still re-synchronize with the grid after around one cycle of oscillation, even if FCA > CCA, as shown in Fig. 22(c). This superior feature prevents the system collapse, which is traditionally caused by the delayed fault clearance.

Fig. 23 further shows the V_o-δ curve of the grid-forming converter by considering the impact of the first-order RPC. It can be seen that V_o is reduced with the increase of δ due to the droop characteristic, which lowers the maximum power transfer capability of the grid-forming converter. Hence, the grid-forming converter is more prone to the loss of equilibrium points with the RPC, and thus, the transient stability is also degraded. However, the abovementioned benefits of the first-order power control still remain when there are equilibrium points, as demonstrated in [24].

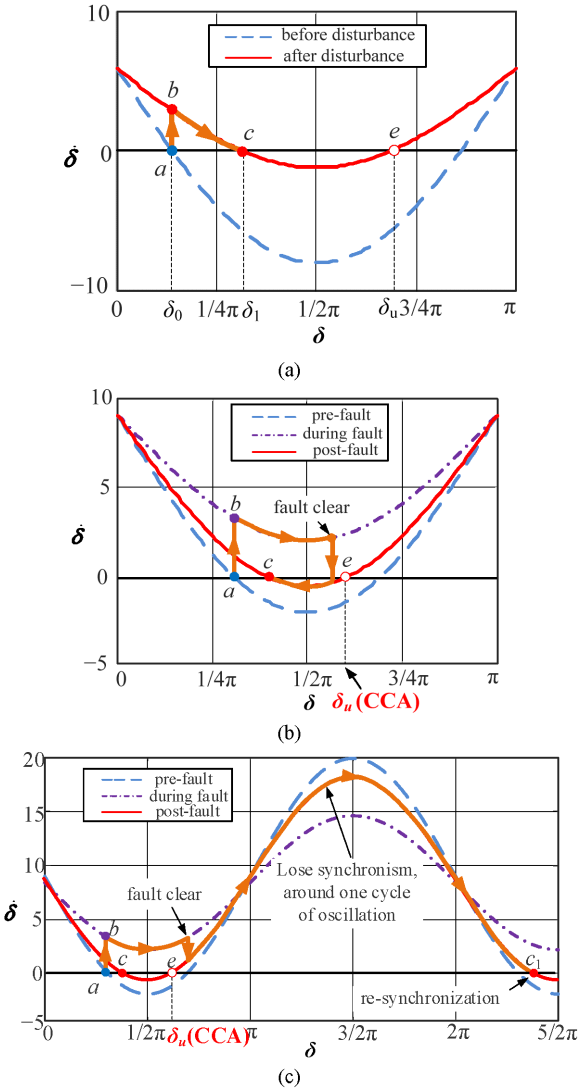

FIGURE 22. Phase portraits of the grid-forming converters with first-order APC. (a) The equilibrium points exist after the transient disturbance. (b) The equilibrium points do not exist during the fault. Fault clearing angle lower than δ_u. (c) The equilibrium points do not exist during the fault. Fault clearing angle higher than δ_u [23].

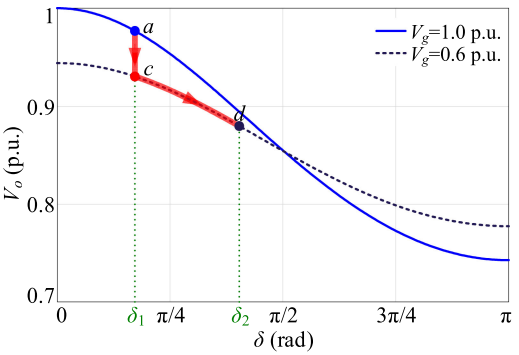

FIGURE 23. V_o-δ curve of the grid-forming converter with the first-order RPC [24].

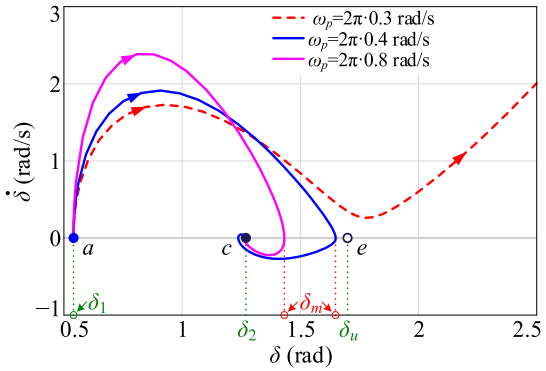

FIGURE 24. Phase portraits of the grid-forming converters with second-order APC [24].

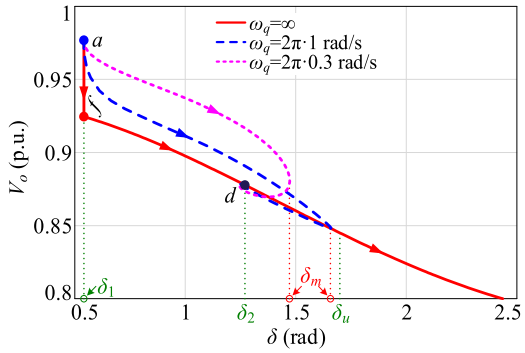

FIGURE 25. V_o-δ curve of the grid-forming converter with the second-order RPC [24].

b) Second-Order Power Angle Control: By adding the LPF into the basic droop control, a second-order power angle dynamics is yielded, as seen in (11), [33]. The second-order APC leads to an underdamped response of the grid-forming converter, which is similar to SGs. Fig. 24 shows the phase portrait of the grid-forming converter with the second-order APC, in which the overshoot in the dynamic response can be observed. The smaller ω_p (or equivalently, larger virtual inertia) enlarges the overshoot, which poses a higher risk of crossing over the UEP, as the red dashed line given by Fig. 24. Hence, although large virtual inertia is supposed to be beneficial to the frequency response of the power system, it jeopardizes the transient stability. Therefore, a tradeoff exists in selecting the virtual inertia [24]. Fig. 25 shows the V_o-δ curve of the grid-forming converter with the second-order RPC, it can be seen that transient voltage drop introduced by the RPC is alleviated by the LPF therein. The smaller cutoff frequency ω_q of the LPF helps to slow down the transient voltage dynamic, which is beneficial for the transient stability of the system.

From the above analysis, it can be concluded that the two LPFs in the active and the reactive power loops take opposite effects on the transient stability, i.e. the former degrades the stability while the latter improves it. The better transient stability performance demands an LPF with a high cutoff frequency (low inertia) in the active power loop and an LPF with a low cutoff frequency in the reactive power loop [24].

TABLE 5. Transient Stability Enhancement Methods for Grid-Forming Converters

Categories	Proposal
Change active and reactive power references	Reducing the active power reference [81]
	Increasing the reactive power reference [82]
Modify control loops or controller parameters	Coordinate the design of virtual inertia and damping term [24]
	Gain scheduled inertia and damping [83]
	Mode- switching control [80]

3) STABILIZING CONTROL METHODS

There are, in general, two categories of control methods for enhancing the transient stability of grid-forming converters, which are summarized in Table 5.

a) Change Active and Reactive Power References: Since grid-forming converters with the second-order power control loops exhibit similar dynamics as SGs, the existing methods for stabilizing SGs, e.g., controlling the governor to reduce the accelerating power and/or injecting additional reactive power to boost the output voltage during grid faults, can be directly adopted. As pointed out in [81], [82], the transient stability of grid-forming converters can also be enhanced by reducing the active power reference and/or increasing the reactive power reference during grid voltage sags, as shown in Fig. 26(a)–(b). The typical challenge of these methods lies in how to quantify the changes of power references, i.e., the selections of n_p and n_q in Fig. 26(a)-(b), which requires the prior knowledge of grid impedance.

b) Modify Control Loops or Controller Parameters: It has been pointed out that the better transient stability performance of grid-forming converter is yielded with the first-order power control. Yet, the inertia emulation is often required, which leads to a second or even higher-order power control loops. In those cases, it is still possible to coordinate the design of virtual inertia and damping terms, in order to approximate the first-order power control dynamics of grid-forming converters, even if higher-order power control loops are used [24]. Besides using the fixed virtual inertia and damping terms [24], the gain-scheduled virtual inertia and damping control for grid-forming converters is reported in [83], where the power control loops only approximate the first-order dynamics during the transient disturbance, as shown in Fig. 26(c).

Differing from the approximated first-order power angle control during the fault, Fig. 26(d) shows the block diagram of a mode-switching control, which is reported in [80], where a control gain k is inserted in the forward path of the control loop, and is switched between $+1$ and -1 based on operating scenarios, such that the positive-feedback dynamics after crossing over the UEP can be avoided. The advantage of the mode-switching control is that no approximation of second-order power control to the first-order one is needed, and the virtual inertia can be tuned in a wide range. Yet, the

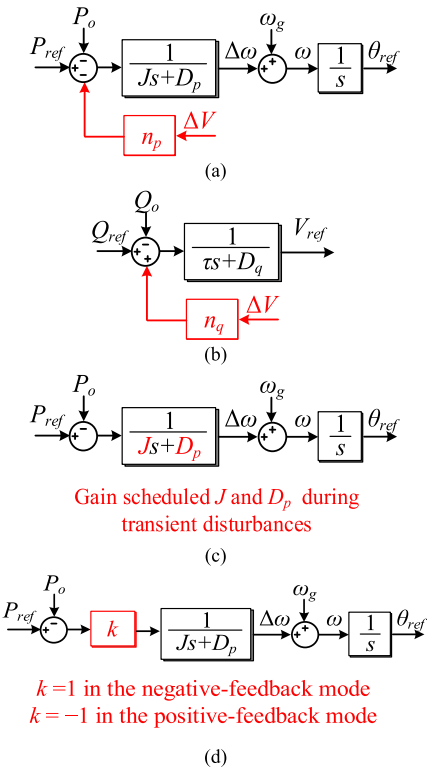

FIGURE 26. Stabilizing control methods. (a) Reduce the active power reference [81]. (b) Increase the reactive power reference [82]. (c) Gain scheduled virtual inertia and damping terms [83]. (d) Mode-switching control [80].

mode-switching control does require a reliable detection of the operating scenarios.

4) CURRENT LIMITING CONTROL

The current limit of grid-forming converters can be triggered during severe faults. In this case, the grid-forming converter will be operated in the current limiting control mode, and its synchronization can be realized by the backup PLL [10], or still based on the APC [84]. In the former case, the grid-forming control turns into the grid-following mode and its transient stability characteristic is detailed in Section III-B. Further, during the fault recovery stage, switching back to the grid-forming control may also cause instability issues [85]. In the latter case, the maximum power transfer capability is reduced due to the current limitation, and the grid-forming converter is prone to the LOS due to the higher risk of loss of equilibrium points [84].

To avoid the switching between the grid-forming and grid-following modes, it is increasingly required to keep the grid-forming mode even during severe grid faults, and to provide an effective current limitation. Several control methods have been developed to meet this requirement, which are listed in Table 6.

It is clear that directly limiting the converter current will leave the converter voltage uncontrolled, resulting in control errors in the outer loops. Hence, the effective current limiting control is often accomplished in the outer loops. In general, the current limitation can be accomplished by using a virtual impedance controller or a modified droop controller. One implementation of this is given in [86], where a grid-forming fault-mode controller including converter current limitation is reported. The power references for outer droop controllers are replaced with the attainable power references based on the measured voltage drop during the fault. In this way, the power-synchronization control still works, and the converter can limit its injected currents without controller saturation and integrator windup. This has the advantage of accurate current limitation but is only developed under symmetrical fault conditions. In [87], the current limitation is achieved by using a virtual resistor, yet the design of the virtual resistance is cumbersome, due to its voltage dependency. In [88], the outer power loops are disabled during faults, and the current is limited through a virtual admittance. This method can limit the converter current during faults, but has the disadvantage of disabling the outer control loops that are needed for the grid-forming operation.

TABLE 6. Methods for Current Limitation for Grid-Forming Converters

Ref.	Proposal
[10], [90]	Switching to a grid-following converter
[86]	Modify outer power references during fault
[87]	Current limitation through virtual resistance
[88]	Disable outer power controllers and limit the current through virtual admittance
[25]	Adaptive parameters for droop controller and virtual impedance
[89]	Enhanced droop control for current limitation
[85]	Using voltage limitation to provide current limitation

The large-signal stability of the post-fault synchronization process of grid-forming converters is analyzed in [25], which uses an adaptive virtual impedance for the current limitation. To enhance the transient stability, the adaptive droop gains based on the voltage amplitude is proposed. A droop control scheme that accounts for the current limitation is reported in [89], which shows improved performance compared to the virtual impedance approach. A current limitation approach through imposing voltage limits is presented in [85]. Despite those methods being able to limit the current and retain the grid-forming mode during the fault, the transient instability may still occur, due to the adoption of second-order APC in those cases. Using the first-order APC together with the current limiting control may yield a better transient stability behavior, as explained in Section IV-B 2. However, the impacts of current limiting control schemes on the transient stability of grid-forming converters still remain as an open issue. Further, the analysis and estimation of the CCA for grid-forming converters with the current limiting control need to be addressed.

V. CONCLUSION

This paper has given a comprehensive review of the grid-synchronization stability of converter-based resources under

weak, stiff and faulty grid conditions. Systematic discussions on instability phenomena, modeling and analysis methods, as well as active stabilization schemes, in regards to both the small- and large-signal synchronization stability, have been presented. In each category, the advantages and drawbacks of grid-following and grid-forming converters are discussed.

A. CHALLENGES WITH GRID CODES

With the increasing share of converter-based resources in power grids, the grid code needs to be continuously updated to maintain the synchronization stability of grid-connected converters. First, it has been identified that the fully reactive current injection during severe grid faults may cause the LOS of converter-based resources. Second, the requirements for voltage and frequency ride-through have been specified in grid codes. Yet, how to ride through the rate of change of the voltage angle in the future converter-dominated power grids still remains an open issue [91]. Third, although grid-forming converters are increasingly demanded by power transmission system operators, there are no grid codes published on the grid-forming capability of converter-based resources [92].

B. PROSPECTS OF FUTURE RESEARCH

To avoid causing the sideband oscillations in low SCR grids, grid-forming converters are increasingly preferred over grid-following converters. However, grid-forming converters tend to be unstable in the stiff and series-compensated grids. More research efforts on the small-signal synchronization stability of grid-forming converters are expected. Further, while the analogies between synchronization dynamics of converters and that of SGs have been established, the unique challenge with converter-based resources is that their synchronization dynamics are highly dependent on their control structure and controller parameters, and hence, a design-oriented analysis plays a critical role in stabilizing converter-based resources. Such design-oriented analysis works well in single converter systems, yet tends to be complicated in power systems with multiple converters. Addressing this challenge requires the development of reduced-order modeling methods for future converter-dominated power grids.

REFERENCES

[1] B. Kroposki *et al.*, "Achieving a 100% renewable grid: Operating electric power systems with extremely high levels of variable renewable energy," *IEEE Power Energy Magn.*, vol. 15, no. 2, pp. 61–73, Mar. 2017.

[2] F. Blaabjerg, R. Teodorescu, M. Liserre, and A. V. Timbus, "Overview of control and grid synchronization for distributed power generation systems," *IEEE Trans. Ind. Electron.*, vol. 53, no. 5, pp. 1398–1409, Oct. 2006.

[3] R. Teodorescu, M. Liserre, and P. Rodriguez, *Grid Converters For Photovoltaic And Wind Power Systems*. Hoboken, NJ, USA: Wiley-IEEE Press, 2011.

[4] A. Luna *et al.*, "Grid voltage synchronization for distributed generation systems under grid fault conditions," *IEEE Trans. Ind. Appl.*, vol. 51, no. 4, pp. 3414–3425, Jul. 2015.

[5] M. Karimi-Ghartemani, "A unifying approach to single-phase synchronous reference frame PLLs," *IEEE Trans. Power Electron.*, vol. 28, no. 10, pp. 4550–4556, Oct. 2013.

[6] X. Wang and F. Blaabjerg, "Harmonic stability in power electronic-based power systems: concept, modeling, and analysis," *IEEE Trans. Smart Grid*, vol. 10, no. 3, pp. 2858–2870, May 2019.

[7] M. G. Taul, X. Wang, P. Davari, and F. Blaabjerg, "An overview of assessment methods for synchronization stability of grid-connected converters under severe symmetrical grid faults," *IEEE Trans. Power Electron.*, vol. 34, no. 10, pp. 9655–9670, Oct. 2019.

[8] National Grid, "Performance of phase-locked loop based converters," System Operability Framework, U.K., Tech. Rep., Dec. 2017.

[9] R. H. Lasseter, Z. Chen, and D. Pattabiraman, "Grid-Forming inverters: A critical asset for the power grid," *IEEE J. Emerg. Sel. Top. Power Electron.*, vol. 8, no. 2, pp. 925–935, Jun. 2020.

[10] L. Zhang, L. Harnefors, and H. Nee, "Power-synchronization control of grid-connected voltage-source converters," *IEEE Trans. Power Syst.*, vol. 25, no. 2, pp. 809–820, May 2010.

[11] J. Machowski, J. W. Bialek, and J. R. Bumby, *Power System Dynamics: Stability And Control*, 2nd ed. Hoboken, NJ, USA: John Wiley Sons.

[12] ENTSO-E, "High penetration of power electronic interfaced power sources and the potential contribution of grid forming converters," Tech. Rep., Jan. 2020.

[13] P. Kundur *et al.*, "Definition and classification of power system stability IEEE/CIGRE joint task force on stability terms and definitions," *IEEE Trans. Power Syst.*, vol. 19, no. 3, pp. 1387–1401, Aug. 2004.

[14] X. Wang, L. Harnefors, and F. Blaabjerg, "Unified impedance model of grid-connected voltage-source converters," *IEEE Trans. Power Electron.*, vol. 33, no. 2, pp. 1775–1787, Feb. 2018.

[15] B. Wen and P. Mattavelli, "Harmonic current analysis of the active front end system in the presence of grid voltage disturbance," in *Proc. IEEE Appl. Power Electron. Conf. Expo.*, 2018, pp. 499–504.

[16] G. Denis, T. Prevost, P. Panciatici, X. Kestelyn, F. Colas, and X. Guillaud, "Improving robustness against grid stiffness, with internal control of an AC voltage-controlled VSC.," in *Proc. IEEE Power Energy Soc. General Meeting*, 2016, pp. 1–5.

[17] Y. Liao, X. Wang, F. Liu, K. Xin, and Y. Liu, "Sub-synchronous control interaction in grid-forming VSCs with droop control," in *Proc. 4th IEEE Workshop Electron. Grid*, 2019, pp. 1–6.

[18] G. Denis, "From grid-following to grid-forming: The new strategy to build 100% power-electronics interfaced transmission system with enhanced transient behavior," Ph.D. Thesis, Ecole Centrale de Lille, Nov. 2017.

[19] S. Wang, Z. Liu, J. Liu, D. Boroyevich, and R. Burgos, "Small-signal modeling and stability prediction of parallel droop-controlled inverters based on terminal characteristics of individual inverters," *IEEE Trans. Power Electron.*, vol. 35, no. 1, pp. 1045–1063, Jan. 2020.

[20] Y. Prabowo, V. M. Iyer, B. Kim, and S. Bhattacharya, "Modeling and stability assessment of single-phase droop controlled solid state transformer," in *Proc. 10th Int. Conf. Power Electron. Asia*, 2019, pp. 3285–3291.

[21] G. Li *et al.*, "Analysis and mitigation of sub-synchronous resonance in series-compensated grid-connected system controlled by virtual synchronous generator," *IEEE Trans. Power Electron.*, vol. 35, no. 10, pp. 11096–11107, Oct. 2020.

[22] H. Wu and X. Wang, "Design-oriented transient stability analysis of PLL-synchronized voltage-source converters," *IEEE Trans. Power Electron.*, vol. 35, no. 4, pp. 3573–3589, Apr. 2020.

[23] H. Wu and X. Wang, "Design-oriented transient stability analysis of grid-connected converters with power synchronization control," *IEEE Trans. Ind. Electron.*, vol. 66, no. 8, pp. 6473–6482, Aug. 2019.

[24] D. Pan, X. Wang, F. Liu, and R. Shi, "Transient stability of voltage-source converters with grid-forming control: A design-oriented study," *IEEE J. Emerg. Sel. Top. Power Electron.*, vol. 8, no. 2, pp. 1019–1033, Jun. 2020.

[25] T. Qoria, F. Gruson, F. Colas, G. Denis, T. Prevost, and X. Guillaud, "Critical clearing time determination and enhancement of grid-forming converters embedding virtual impedance as current limitation algorithm," *IEEE J. Emerg. Sel. Top. Power Electron.*, vol. 8, no. 2, pp. 1050–1061, Jun. 2020.

[26] J. Rocabert, A. Luna, F. Blaabjerg, and P. Rodríguez, "Control of power converters in AC Microgrids," *IEEE Trans. Power Electron.*, vol. 27, no. 11, pp. 4734–4749, Nov. 2012.

[27] D. Dong, B. Wen, D. Boroyevich, P. Mattavelli, and Y. Xue, "Analysis of phase-locked loop low-frequency stability in three-phase grid-connected power converters considering impedance interactions," *IEEE Trans. Ind. Electron.*, vol. 62, no. 1, pp. 310–321, Jan. 2015.

[28] Y. Li, D. M. Vilathgamuwa, and P. C. Loh, "Design, analysis, and real-time testing of a controller for multibus microgrid system," *IEEE Trans. Power Electron.*, vol. 19, no. 5, pp. 1195–1204, Sep. 2004.

[29] P. Rodriguez, I. Candela, and A. Luna, "Control of PV generation systems using the synchronous power controller," in *Proc. IEEE Energy Convers. Congr. Expo.*, 2013, pp. 993–998.

[30] N. Pogaku, M. Prodanovic, and T. C. Green, "Modeling, analysis and testing of autonomous operation of an inverter-based microgrid," *IEEE Trans. Power Electron.*, vol. 22, no. 2, pp. 613–625, Mar. 2007.

[31] H. Wu *et al.*, "Small-signal modeling and parameters design for virtual synchronous generators," *IEEE Trans. Ind. Electron.*, vol. 63, no. 7, pp. 4292–4303, Jul. 2016.

[32] Q. Zhong and G. Weiss, "Synchronverters: Inverters that mimic synchronous generators," *IEEE Trans. Ind. Electron.*, vol. 58, no. 4, pp. 1259–1267, Apr. 2011.

[33] S. D' Arco and J. A. Suul, "Equivalence of virtual synchronous machines and frequency-droops for converter-based microgrids," *IEEE Trans. Smart Grid*, vol. 5, no. 1, pp. 394–395, Jan. 2014.

[34] S. Dong and Y. C. Chen, "Adjusting synchronverter dynamic response speed via damping correction loop," *IEEE Trans. Energy Convers.*, vol. 32, no. 2, pp. 608–619, 2017.

[35] D. Chen, Y. Xu, and A. Q. Huang, "Integration of dc microgrids as virtual synchronous machines into the AC grid," *IEEE Trans. Ind. Electron.*, vol. 64, no. 9, pp. 7455–7466, 2017.

[36] Ö. Göksu, R. Teodorescu, C. L. Bak, F. Iov, and P. C. Kjær, "Instability of wind turbine converters during current injection to low voltage grid faults and PLL frequency based stability solution," *IEEE Trans. Power Syst.*, vol. 29, no. 4, pp. 1683–1691, Jul. 2014.

[37] D. Dong, J. Li, D. Boroyevich, P. Mattavelli, I. Cvetkovic, and Y. Xue, "Frequency behavior and its stability of grid-interface converter in distributed generation systems," in *Proc. 27th Annu. IEEE Appl. Power Electron. Conf. Expo.*, 2012, pp. 1887–1893.

[38] L. Harnefors, X. Wang, A. G. Yepes, and F. Blaabjerg, "Passivity-based stability assessment of grid-connected VSCs—an overview," *IEEE J. Emerg. Sel. Top. Power Electron*., vol. 4, no. 1, pp. 116–125, Mar. 2016.

[39] D. Yang, X. Wang, F. Liu, K. Xin, Y. Liu, and F. Blaabjerg, "Symmetrical PLL for SISO impedance modeling and enhanced stability in weak grids," *IEEE Trans. Power Electron.*, vol. 35, no. 2, pp. 1473–1483, Feb. 2020.

[40] J. Z. Zhou, H. Ding, S. Fan, Y. Zhang, and A. M. Gole, "Impact of short-circuit ratio and phase-locked-loop parameters on the small-signal behavior of a VSC-HVDC converter," *IEEE Trans. Power Del.*, vol. 29, no. 5, pp. 2287–2296, Oct. 2014.

[41] D. Yang and X. Wang, "Unified modular state-space modeling of grid-connected voltage-source converters," *IEEE Trans. Power Electron.*, vol. 35, no. 9, pp. 9700–9715, Sep. 2020.

[42] Y. Liao and X. Wang, "Impedance-based stability analysis for interconnected converter systems with open-loop RHP poles," *IEEE Trans. Power Electron.*, vol. 35, no. 4, pp. 4388–4397, Apr. 2020.

[43] L. Harnefors, M. Bongiorno, and S. Lundberg, "Input-admittance calculation and shaping for controlled voltage-source converters," *IEEE Trans. Ind. Electron.*, vol. 54, no. 6, pp. 3323–3334, Dec. 2007.

[44] C. Zhang, X. Cai, A. Rygg, and M. Molinas, "Sequence domain SISO equivalent models of a grid-tied voltage source converter system for small-signal stability analysis," *IEEE Trans. Energy Convers.*, vol. 33, no. 2, pp. 741–749, Jun. 2018.

[45] S.-F. Chou, X. Wang, and F. Blaabjerg, "Two-port network modeling and stability analysis of grid-connected current-controlled VSCs," *IEEE Trans. Power Electron.*, vol. 35, no. 4, pp. 3519–3529, Apr. 2020.

[46] B. Wen, D. Boroyevich, R. Burgos, P. Mattavelli, and Z. Shen, "Analysis Of D-Q small-signal impedance of grid-tied inverters," *IEEE Trans. Power Electron.*, vol. 31, no. 1, pp. 675–687, Jan. 2016.

[47] K. M. Alawasa, Y. A. I. Mohamed, and W. Xu, "Active mitigation of subsynchronous interactions between PWM voltage-source converters and power networks," *IEEE Trans. Power Electron.*, vol. 29, no. 1, pp. 121–134, Jan. 2014.

[48] J. A. Suul, S. D'Arco, P. Rodríguez, and M. Molinas, "Impedance-compensated grid synchronisation for extending the stability range of weak grids with voltage source converters," *IET Generation Transmiss. Distrib.*, vol. 10, no. 6, pp. 1315–1326, May 2016.

[49] J. Fang, X. Li, H. Li, and Y. Tang, "Stability improvement for three-phase grid-connected converters through impedance reshaping in quadrature-axis," *IEEE Trans. Power Electron.*, vol. 33, no. 10, pp. 8365–8375, Oct. 2018.

[50] X. Zhang, D. Xia, Z. Fu, G. Wang, and D. Xu, "An improved feedforward control method considering PLL dynamics to improve weak grid stability of grid-connected inverters," *IEEE Trans. Ind. Appl.*, vol. 54, no. 5, pp. 5143–5151, Sep. 2018.

[51] X. Zhang, S. Fu, W. Chen, N. Zhao, G. Wang, and D. G. Xu, "A symmetrical control method for grid-connected converters to suppress the frequency coupling under weak grid conditions," *IEEE Trans. Power Electron.*, vol. 35, no. 12, pp. 13488–13499, Dec. 2020.

[52] L. Zhang, L. Harnefors, and H. Nee, "Interconnection of two very weak AC systems by VSC-HVDC links using power-synchronization control," *IEEE Trans. Power Syst.*, vol. 26, no. 1, pp. 344–355, Feb. 2011.

[53] M. G. Taul, X. Wang, P. Davari, and F. Blaabjerg, "An efficient reduced-order model for studying synchronization stability of grid-following converters during grid faults," in *Proc. IEEE 20th Workshop Control Model. Power Electron*, 2019, pp. 1–7.

[54] X. He, H. Geng, and S. Ma, "Transient stability analysis of grid-tied converters considering PLL's nonlinearity," *CPSS Trans. Power Electron. Appl.*, vol. 4, no. 1, pp. 40–49, Mar. 2019.

[55] Q. Hu, J. Hu, H. Yuan, H. Tang, and Y. Li, "Synchronizing stability of DFIG-based wind turbines attached to weak AC grid," in *Proc. 17th Int. Conf. Elect. Mach. Syst.*, 2014, pp. 2618–2624.

[56] Q. Hu, L. Fu, F. Ma, and F. Ji, "Large signal synchronizing instability of PLL-based VSC connected to weak AC grid," *IEEE Trans. Power Syst.*, vol. 34, no. 4, pp. 3220–3229, Jul. 2019.

[57] F. Andrade, K. Kampouropoulos, L. Romeral, J. C. Vasquez, and J. M. Guerrero, "Study of large-signal stability of an inverter-based generator using a Lyapunov function," in *Proc. 40th Annu. Conf. IEEE Ind. Electron. Soc.*, 2014, pp. 1840–1846.

[58] M. Huang, Y. Peng, C. K. Tse, Y. Liu, J. Sun, and X. Zha, "Bifurcation and large-signal stability analysis of three-phase voltage source converter under grid voltage dips," *IEEE Trans. Power Electron.*, vol. 32, no. 11, pp. 8868–8879, Nov. 2017.

[59] M. G. Taul, X. Wang, P. Davari, and F. Blaabjerg, "Systematic approach for transient stability evaluation of grid-tied converters during power system faults," in *Proc. IEEE Energy Convers. Congr. Expo.*, 2019, pp. 5191–5198.

[60] I. Erlich, F. Shewarega, S. Engelhardt, J. Kretschmann, J. Fortmann, and F. Koch, "Effect of wind turbine output current during faults on grid voltage and the transient stability of wind parks," in *Proc. IEEE Power Energy Soc. Generation Meeting*, 2009, pp. 1–8.

[61] H. Geng, L. Liu, and R. Li, "Synchronization and reactive current support of PMSG-based wind farm during severe grid fault," *IEEE Trans. Sustain. Energy*, vol. 9, no. 4, pp. 1596–1604, Oct. 2018.

[62] S. Ma, H. Geng, L. Liu, G. Yang, and B. C. Pal, "Grid-synchronization stability improvement of large scale wind farm during severe grid fault," *IEEE Trans. Power Syst*., vol. 33, no. 1, pp. 216–226, Jan. 2018.

[63] X. He, H. Geng, R. Li, and B. C. Pal, "Transient stability analysis and enhancement of renewable energy conversion system during LVRT," *IEEE Trans. Sustain. Energy*, vol. 11, no. 3, pp. 1612–1623, Jul. 2019.

[64] A. B. V. Diedrichs and S. Adloff, "Loss of (angle) stability of wind power plants - the underestimated phenomenon in case of very low circuit ratio," in *Proc. 10th Int. Workshop Large-Scale Integration Wind Power Into Power Syst. As Well As Transmiss. Netw. Offshore Wind Farms*, pp. 395–402.

[65] R. E. Betz and M. Graungaard Taul, "Identification of grid impedance during severe faults," in *Proc. IEEE Energy Convers. Congr. Expo.*, 2019, pp. 1076–1082.

[66] M. G. Taul, X. Wang, P. Davari, and F. Blaabjerg, "Robust fault ride through of converter-based generation during severe faults with phase jumps," *IEEE Trans. Ind. Appl*., vol. 56, no. 570–583, Jan. 2020.

[67] B. Weise, "Impact of K-factor and active current reduction during fault-ride-through of generating units connected via voltage-sourced converters on power system stability," *IET Renew. Power Generation*, vol. 9, no. 1, pp. 25–36, Jan. 2015.

[68] H. Wu and X. Wang, "Transient stability impact of the phase-locked loop on grid-connected voltage source converters," in *Proc. Int. Power Electron. Conf.*, 2018, pp. 2673–2680.

[69] H. Wu and X. Wang, "An Adaptive phase-locked loop for the transient stability enhancement of grid-connected voltage source converters," in *Proc. IEEE Energy Convers. Congr. Expo.*, 2018, pp. 5892–5898.

[70] H. Wu and X. Wang, "Transient angle stability analysis of grid-connected converters with the first-order active power loop," in *Proc. IEEE Appl. Power Electron. Conf. Expo.*, 2018, pp. 3011–3016.

[71] D. Yang, H. Wu, X. Wang, and F. Blaabjerg, "Suppression of synchronous resonance for VSGs," *J. Eng.*, vol. 2017, no. 13, pp. 2574–2579, 2017.
[72] X. Li, Y. Hu, Y. Shao, and G. Chen, "Mechanism analysis and suppression strategies of power oscillation for virtual synchronous generator," in *Proc. 43rd Annu. Conf. IEEE Ind. Electron. Soc.*, 2017, pp. 4955–4960.
[73] J. Wang, Y. Wang, Y. Gu, W. Li, and X. He, "Synchronous frequency resonance of virtual synchronous generators and damping control," in *Proc. 9th Int. Conf. Power Electron. Asia*, 2015, pp. 1011–1016.
[74] P. R. Cortes, J. L. C. Garcia, J. R. Delgador, and R. Teodorescu, "Virtual controller of electromechanical characteristics for static power converters," European Patent Application: EP 2 683 075 A1, 2014.
[75] G. N. Baltas, N. B. Lai, L. Marin, A. Tarraso, and P. Rodriguez, "Grid-forming power converters tuned through artificial intelligence to damp subsynchronous interactions in electrical grids," *IEEE Access*, vol. 8, pp. 93369–93379, 2020.
[76] Y. Tao, Y. Deng, G. Li, G. Chen, and X. He, "Evaluation and comparison of the low-frequency oscillation damping methods for the droop-controlled inverters in distributed generation systems," *J. Power Electron.*, vol. 16, no. 2, pp. 731–747, Mar. 2016.
[77] M. M. Esfahani, H. F. Habib, and O. A. Mohammed, "Microgrid stability improvement using a fuzzy-based PSS design for virtual synchronous generator," in *Proc. SoutheastCon*, 2018, pp. 1–5.
[78] A. W. Korai and I. Erlich, "Frequency dependent voltage control by DER units to improve power system frequency stability," in *Proc. IEEE Eindhoven Power Tech, PowerTech*, 2015, pp. 1–6.
[79] X. Wang, Y. W. Li, F. Blaabjerg, and P. C. Loh, "Virtual-impedance-based control for voltage-source and current-source converters," *IEEE Trans. Power Electron.*, vol. 30, no. 12, pp. 7019–7037, Dec. 2015.
[80] H. Wu and X. Wang, "A mode-adaptive power-angle control method for transient stability enhancement of virtual synchronous generators," *IEEE J. Emerg. Sel. Top. Power Electron.*, vol. 8, no. 2, pp. 1034–1049, Jun. 2020.
[81] Z. Shuai, C. Shen, X. Liu, Z. Li, and Z. J. Shen, "Transient angle stability of virtual synchronous generators using Lyapunov's direct method," *IEEE Trans. Smart Grid*, vol. 10, no. 4, pp. 4648–4661, Jul. 2019.
[82] D. Pan, X. Wang, F. Liu, and R. Shi, "Transient stability impact of reactive power control on grid-connected converters," in *Proc. IEEE Energy Convers. Congr. Expo.*, 2019, pp. 4311–4316.
[83] J. Alipoor, Y. Miura, and T. Ise, "Power system stabilization using virtual synchronous generator with alternating moment of inertia," *IEEE J. Emerg. Sel. Top. Power Electron.*, vol. 3, no. 2, pp. 451–458, Jun. 2015.
[84] L. Huang, H. Xin, Z. Wang, L. Zhang, K. Wu, and J. Hu, "Transient stability analysis and control design of droop-controlled voltage source converters considering current limitation," *IEEE Trans. Smart Grid*, vol. 10, no. 1, pp. 578–591, Jan. 2019.
[85] J. Chen, F. Prystupczuk, and T. O'Donnell, "Use of voltage limits for current limitations in grid-forming converters," *CSEE J. Power Energy Syst.*, vol. 6, no. 2, pp. 259–269, Jun. 2020.
[86] M. G. Taul, X. Wang, P. Davari, and F. Blaabjerg, "Current limiting control with enhanced dynamics of grid-forming converters during fault conditions," *IEEE J. Emerg. Sel. Top. Power Electron*., vol. 8, no. 2, pp. 1062–1073, Jun. 2019.
[87] C. Glockler, D. Duckwitz, and F. Welck, "Virtual synchronous machine control with virtual resistor for enhanced short circuit capability," in *Proc. IEEE PES Innovative Smart Grid Technol. Conf. Eur.*, 2017, pp. 1–6.
[88] K. Shi, H. Ye, P. Xu, D. Zhao, and L. Jiao, "Low-voltage ride through control strategy of virtual synchronous generator based on the analysis of excitation state," *IET Generation Transmiss. Distrib.*, vol. 12, no. 9, pp. 2165–2172, May 2018.
[89] D. Groß and F. Dörfler, "Projected grid-forming control for current-limiting of power converters," in *Proc. 57th Annu. Allerton Conf. Commun., Control, Comput.*, 2019, pp. 326–333.
[90] K. Shi, W. Song, P. Xu, R. Liu, Z. Fang, and Y. Ji, "Low-voltage ride-through control strategy for a virtual synchronous generator based on smooth switching," *IEEE Access*, vol. 6, pp. 2703–2711, Dec. 2018.
[91] National Grid ESO, "Stability pathfinder RFI – Technical performance and assessment criteria (Attachment 1)," Tech. Rep., Nov. 2019.
[92] National Grid ESO, Draft Grid Code – Grid Forming Converter Specification, Dec. 2019.

XIONGFEI WANG (Senior Member, IEEE) received the B.S. degree from Yanshan University, Qinhuangdao, China, in 2006, the M.S. degree from the Harbin Institute of Technology, Harbin, China, in 2008, both in electrical engineering, and the Ph.D. degree in energy technology from Aalborg University, Aalborg, Denmark, in 2013.

Since 2009, he has been with the Department of Energy Technology, Aalborg University, where he became an Assistant Professor in 2014, an Associate Professor in 2016, a Professor and Research Program Leader for Electronic Power Grid (eGrid) in 2018, and the Director of Aalborg University-Huawei Energy Innovation Center in 2020. He is also a Visiting Professor of power electronics systems with the KTH Royal Institute of Technology, Stockholm, Sweden. His current research interests include modeling and control of grid-interactive power converters, stability and power quality of power-electronic-based power systems, active and passive filters.

Dr. Wang was selected into Aalborg University Strategic Talent Management Program in 2016. He has received six Prize Paper Awards in the IEEE Transactions and conferences, the 2016 Outstanding Reviewer Award of IEEE Transactions on Power Electronics, the 2018 IEEE PELS Richard M. Bass Outstanding Young Power Electronics Engineer Award, the 2019 IEEE PELS Sustainable Energy Systems Technical Achievement Award, the 2019 Highly Cited Researcher by Clarivate Analytics (former Thomson Reuters), and the 2020 IEEE PES Prize Paper Award. He serves as a Member-at-Large for Administrative Committee of IEEE Power Electronics Society in 2020-2022, and as an Associate Editor for the IEEE TRANSACTIONS ON POWER ELECTRONICS, the IEEE TRANSACTIONS ON INDUSTRY APPLICATIONS, and the IEEE JOURNAL OF EMERGING AND SELECTED TOPICS IN POWER ELECTRONICS.

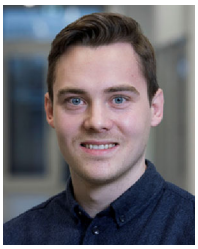

MADS GRAUNGAARD TAUL (Member, IEEE) received the B.Sc. and M.Sc. degrees in electrical energy engineering with a specialization in power electronics and drives in 2016 and 2019, respectively, and the Ph.D. degree in power electronic systems from Aalborg University, Denmark in 2020. Dr. Taul was a Visiting Researcher at the University of California, Berkeley, at the Department of Electrical Engineering and Computer Science from August 2019 to January 2020. Currently, he is a Postdoctoral Researcher with the Department of Energy Technology at Aalborg University, Denmark. In connection with his M.Sc. degree, he received the 1st Prize Master's Thesis Award for excellent and innovative project work by the Energy Sponsor Programme. His main research interests include renewable energy sources and grid-connected converters with a particular focus on modeling, control, and stability analysis of power electronics-based power systems.

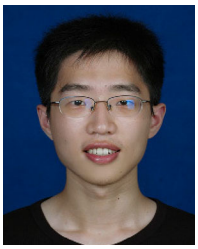

HENG WU (Member, IEEE) received the B.S. and M.S. degrees in electrical engineering from the Nanjing University of Aeronautics and Astronautics (NUAA), Nanjing, China, in 2012 and 2015, respectively, and the Ph.D. degree in energy technology from Aalborg University, Aalborg, Denmark, in 2020. He is now a Postdoctoral Researcher with the Department of Energy Technology, Aalborg University. From 2015 to 2017, he was an Electrical Engineer with NR Electric Co., Ltd, Nanjing, China. He was a Guest Researcher with Ørsted Wind Power, Fredericia, Denmark, from November to December 2018, and with Bundeswehr University Munich, Germany, from September to December, 2019. He received the 2019 Outstanding Reviewer Award of the IEEE TRANSACTIONS ON POWER ELECTRONICS. His research interests include the modelling and stability analysis of the power electronic based power systems.

YICHENG LIAO (Student Member, IEEE) received the B.S. degree in electrical engineering and automation and the M.S. degree in electrical engineering from Southwest Jiaotong University, Chengdu, China, in 2015 and 2018, respectively. She is currently working torward the Ph.D. degree in power electronic engineering in Aalborg University, Aalborg, Denmark. She was a Visiting Student with Ecole Polytechnique and French National Institute for Research in Digital Science and Technology, Paris, France, in July 2017, and has been a Research Assistant with the Department of Energy Technology, Aalborg University since September 2018. Her research interests include the modeling, stability analysis, and control of power electronics-based power systems.

FREDE BLAABJERG (Fellow, IEEE) was with ABB-Scandia, Randers, Denmark, from 1987 to 1988. From 1988 to 1992, he got the Ph.D. degree in electrical engineering at Aalborg University in 1995. He became an Assistant Professor in 1992, an Associate Professor in 1996, and a Full Professor of power electronics and drives in 1998. From 2017 he became a Villum Investigator. He is honoris causa at University Politehnica Timisoara (UPT), Romania and Tallinn Technical University (TTU) in Estonia.

His current research interests include power electronics and its applications such as in wind turbines, PV systems, reliability, harmonics and adjustable speed drives. He has published more than 600 journal papers in the fields of power electronics and its applications. He is the Co-Author of four monographs and Editor of ten books in power electronics and its applications.

He has received 32 IEEE Prize Paper Awards, the IEEE PELS Distinguished Service Award in 2009, the EPE-PEMC Council Award in 2010, the IEEE William E. Newell Power Electronics Award 2014, the Villum Kann Rasmussen Research Award 2014, the Global Energy Prize in 2019 and the 2020 IEEE Edison Medal. He was the Editor-in-Chief of the IEEE TRANSACTIONS ON POWER ELECTRONICS from 2006 to 2012. He has been Distinguished Lecturer for the IEEE Power Electronics Society from 2005 to 2007 and for the IEEE Industry Applications Society from 2010 to 2011 as well as 2017 to 2018. In 2019-2020 he serves the President of IEEE Power Electronics Society. He is Vice-President of the Danish Academy of Technical Sciences too.

He is nominated in 2014-2019 by Thomson Reuters to be between the most 250 cited researchers in engineering in the world.

LENNART HARNEFORS (Fellow, IEEE) received the M.Sc., Licentiate, and Ph.D. degrees in electrical engineering from the Royal Institute of Technology (KTH), Stockholm, Sweden, and the Docent (D.Sc.) degree in industrial automation from Lund University, Lund, Sweden, in 1993, 1995, 1997, and 2000, respectively.

Between 1994-2005, he was with Mälardalen University, Västerås, Sweden, from 2001 as a Professor of electrical engineering. Between 2001-2005, he was, in addition, a part-time Visiting Professor of electrical drives with the Chalmers University of Technology, Göteborg, Sweden. In 2005, he joined ABB, HVDC Product Group, Ludvika, Sweden, where, among other duties, he led the control development of the first generation of multilevel-converter HVDC Light. In 2012, he joined ABB, Corporate Research, Västerås, where he was appointed as a Senior Principal Scientist in 2013. In this capacity he coordinates ABB's research in control of power electronic systems. He is, in addition, a part-time Adjunct Professor of power electronics with KTH.

Dr. Harnefors is an Associate Editor of the IEEE JOURNAL OF EMERGING AND SELECTED TOPICS IN POWER ELECTRONICS and of *IET Electric Power Applications*. His research interests include control and dynamic analysis of power electronic systems, particularly grid-connected converters and ac drives.